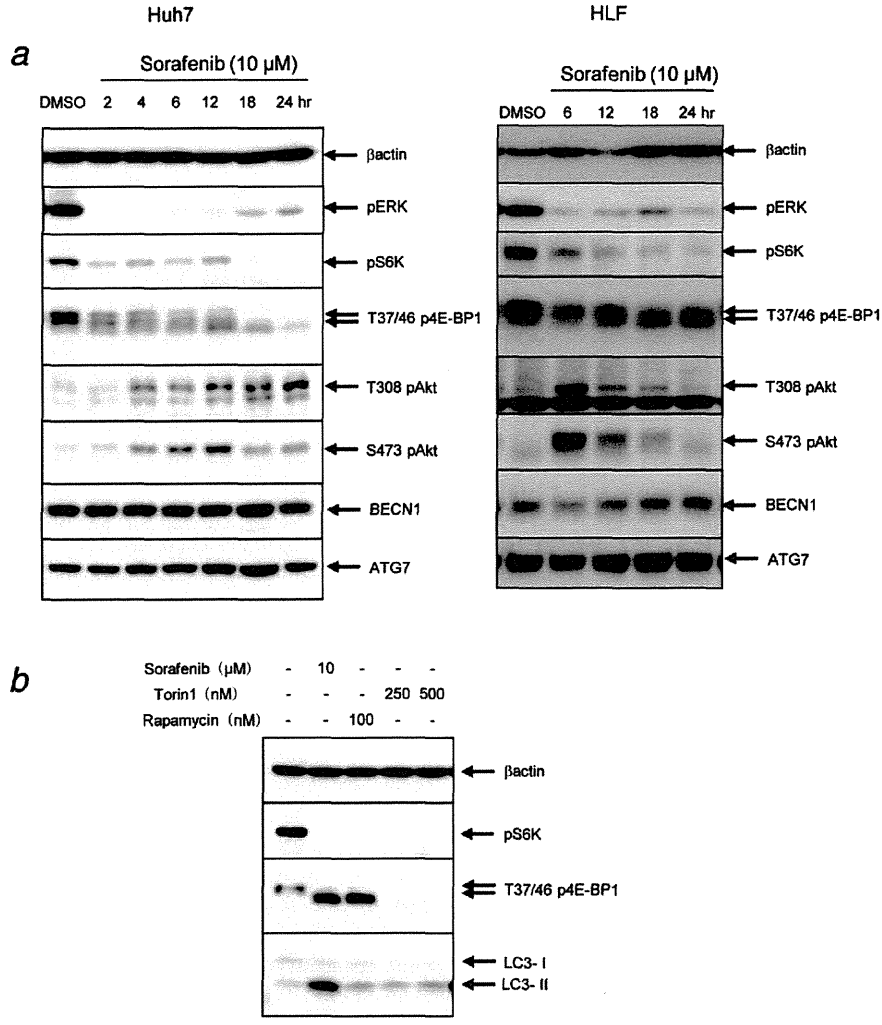

Figure 3. Raf/MEK/ERK and Akt/mTOR/S6K pathways in hepatoma cells treated with sorafenib. (*a*). Western blot showing decrease in ERK, S6K and 4E-BP1 phosphorylation, increase in Akt phosphorylation and stable expression of Beclin 1 and ATG7 in Huh7 cells and HLF cells after treatment with 10 μM sorafenib. (*b*). Western blot showing that rapamycin or Torin1 dephosphorylates both S6K and 4E-BP1 and increases the expression of LC3-II in Huh7 cells. Huh7 cells were treated with 100 nM rapamycin or the indicated concentration of Torin1 for 12 hr. Huh7 treated with sorafenib (10 μM, 12 hr) serves as a positive control. [Color figure can be viewed in the online issue, which is available at wileyonlinelibrary.com.]

administration of sorafenib alone (Fig. 6*b*). Administration of chloroquine alone did not affect the growth of the tumor. We performed TUNEL staining and immunohistological staining of cleaved caspase-3 of the xenograft tumor to examine the contribution of apoptosis in this xenograft model. However, nonspecific staining of the xenograft tumors treated with sorafenib interfered with an accurate evaluation of the apoptotic change (data not shown).

Discussion

Accumulating evidence indicates that cancer therapies such as irradiation and administration of cytotoxic drugs and chemicals induce autophagy and autophagic cell death in a variety of tumor cells.[8] Research has shown that autophagy induced by these treatments sometimes protects tumor cells (autophagic resistance) but promotes cell death in other settings (autophagic Type II programmed cell death). For example, temozolomide, a DNA alkylating agent,[24] and ionizing radiation[25] induce autophagy in malignant glioma cells and a variety of epithelial tumors, respectively, and this inhibition enhances antitumor effects. On the other hand, poly(dI:dC) induces endosome-mediated autophagy leading to cell death in melanoma cells.[26] Arsenic trioxide induces autophagic cell death in leukemia cells.[27] In the present study, we demonstrated that sorafenib, a recently approved molecular targeting drug for HCC, induced autophagy which appeared to

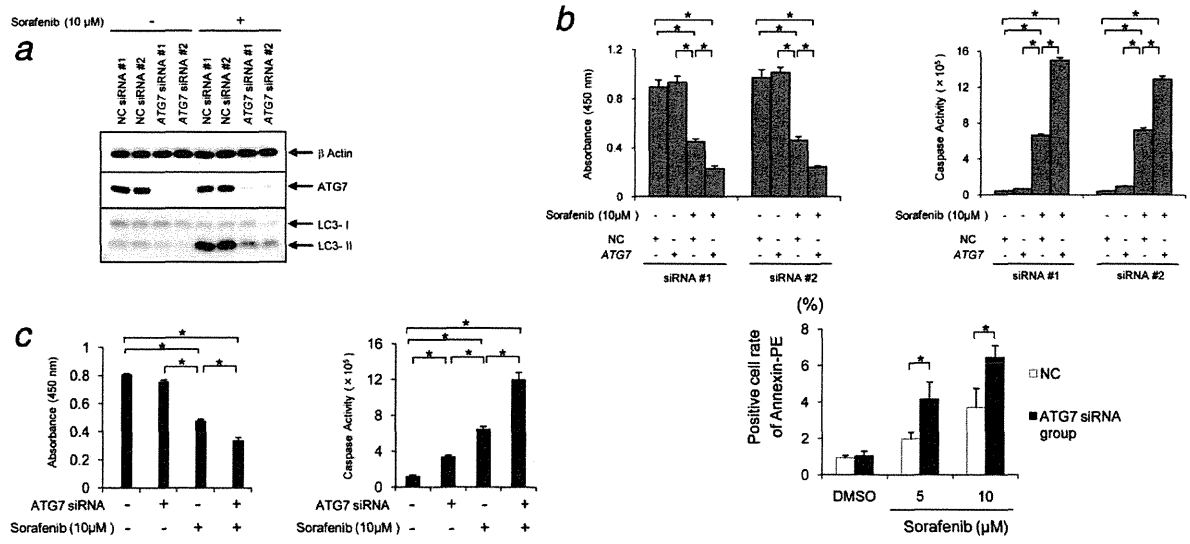

Figure 4. Genetic ablation of autophagy increases sensitivity of hepatoma cells to sorafenib. (*a*,*b*). Huh7 cells were transfected with two different sets of *ATG7* siRNA (no. 1 and 2) or control siRNA (no. 1 and 2) for 48 hr and then treated with the indicated concentration of sorafenib or vehicle for an additional 18 hr. LC3 lipidation and ATG7 expression were determined by western blot (*a*). Cell growth was determined by WST assay, while apoptosis was monitored by the activity of caspase-3/7 in the supernatant or by annexin V positive cell rate ($n = 4$) (*b*). (*c*) HLF cells were transfected with *ATG7* siRNA and examined for cell viability and caspase-3/7 activity in the same manner as Huh7 cells ($n = 4$). *$p < 0.05$. [Color figure can be viewed in the online issue, which is available at wileyonlinelibrary.com.]

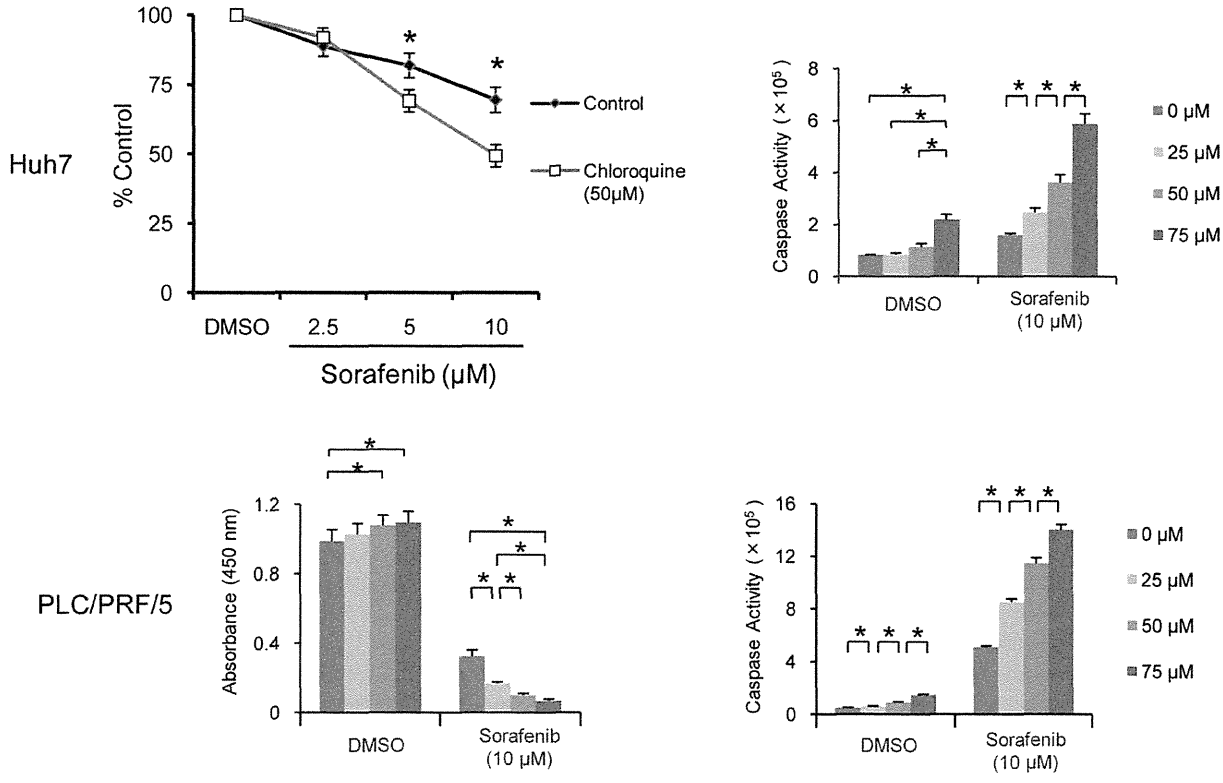

Figure 5. Pharmacological inhibition of autophagy increases sensitivity of hepatoma cells to sorafenib. Huh7 cells or PLC/PRF/5 cells were treated with or without the indicated concentration of sorafenib in the presence or absence of chloroquine for 18 hr. Capsase-3/7 activity was monitored in the supernatant, while cell growth was determined by WST assay ($n = 4$). *$p < 0.05$.

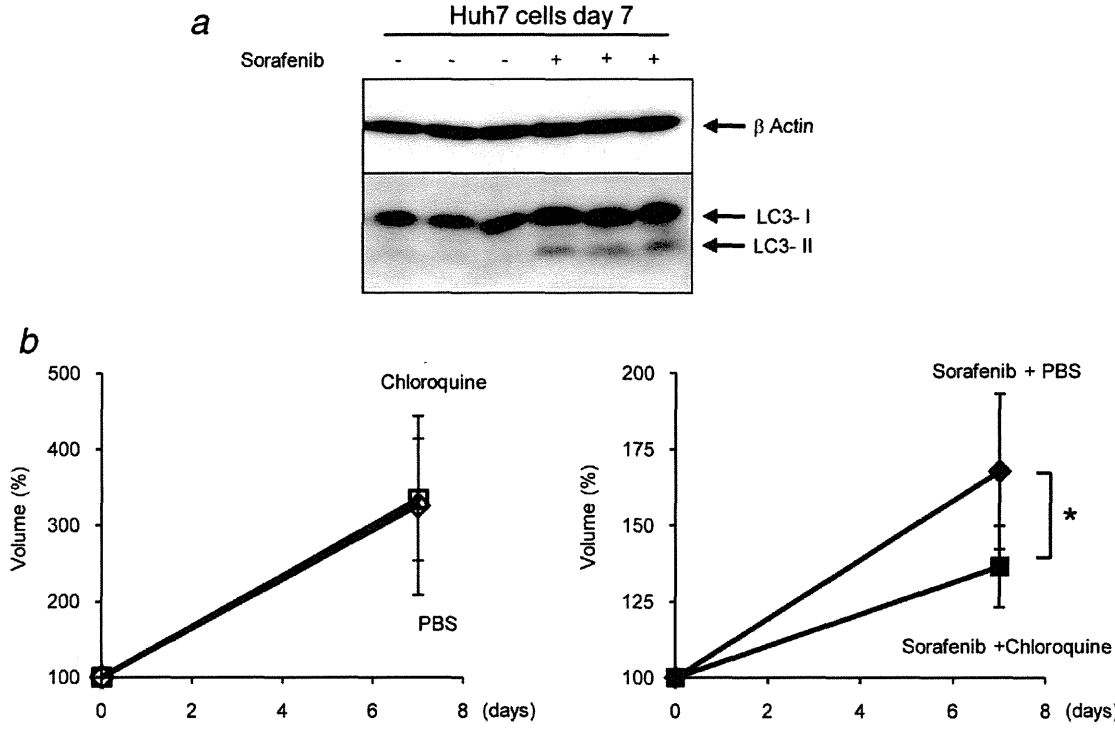

Figure 6. Inhibition of autophagy potentiates sorafenib-induced antitumor effects in Huh7 xenograft. (*a*). Western blot showing increase in LC3-II expression in Huh7 xenograft tumor after sorafenib therapy. Mice bearing xenograft tumor were administered sorafenib (30 mg kg^{-1}) or vehicle for 7 days ($n = 3$/group). (*b*). Chloroquine (60 mg kg^{-1}) itself did not affect the tumor growth of Huh7 xenograft (left panel), ($n = 7$/group), but enhanced the effect of sorafenib (30 mg kg^{-1}) in a synergistic manner (right panel), ($n = 6$/group). Mice bearing xenograft tumor were administered sorafenib and/or chloroquine for 7 days. Tumor volume at 7 days is shown as a percentage of that before initiation of the therapy. *$p < 0.05$. [Color figure can be viewed in the online issue, which is available at wileyonlinelibrary.com.]

promote survival of hepatoma cells and thereby may be a cellular adaptive response related to primary resistance to this compound.

LC3 lipidation and its association with the isolation membranes have been established as useful signs for autophagy detectable by immunoblotting and fluorescence microscopy, facilitating research on autophagy. Previous research has shown that sorafenib induces GFP-LC3 punctate structure and LC3-II conversion in tumor cells.[9–11] However, these techniques should be analyzed more carefully, because positive results clearly indicate increased numbers of autophagosomes but do not always mean upregulation of autophagic flux.[28] For example, treatment with vinblastine or nocodazole leads to LC3 conversion and produces GFP-LC3 punctate structures, resulting from blockade of the fusion of autophagosomes and lysosomes but not from autophagy induction.[29,30] In the present study, we applied several methods including LC3 turnover assay using a lysosomal inhibitor of chloroquine or bafilomycin A1, measurement of the amount of a selective autophagy substrate p62, and observation of the mRFP-GFP color change using a fluorescent-tagged LC3 probe, to obtain evidence showing that sorafenib not only increases the number of autophagosomes but also activates the autophagic flux.

The underlying mechanisms by which sorafenib induces autophagy are not completely clear at present. In addition to the well-known target Raf/MEK/MAPK pathway, sorafenib clearly inhibited the mTORC1 pathway in the present study. Because mTOR inhibition by rapamycin or Torin1 activates autophagosome formation in hepatoma cells, sorafenib-induced inhibition of the mTORC1 pathway might be involved in sorafenib-mediated induction of autophagy. Recently, a putative tumor-suppressor gene *p53* has been shown to transactivate an autophagy-inducing gene, *dram*,[31] and *p53*-dependent induction of autophagy has been documented in response to DNA damage or reexpression of p53 in p53-negative tumor cells.[32] Because the hepatoma cells used in the present study (Huh7, HLF and PLC/PRF/5) possess mutant *p53*, sorafenib-induced adaptive autophagy could occur independently of p53. This finding may be important, because more than half of advanced HCC cases are p53-defective.[33] In such cases, our observations could be applicable and relevant.

Study of rodent carcinogenesis has revealed that autophagic protein degradation is reduced in HCC.[34] In human,

malignant HCC cell lines and HCC tissue with recurrent disease display lower autophagic activity with decreased expression of Beclin 1.[35] The autophagic pathway contributes to the growth-inhibitory effect of TGF-beta in hepatoma cells.[36] Taken together, these findings suggest that defects in autophagy may promote development or progression of HCC, focusing on the tumor suppressive or antitumor effect of autophagy in the liver or HCC. In contrast, the present study clearly showed that autophagy induced by sorafenib protects hepatoma cells from apoptotic cell death, thus shedding light on the tumor-promoting effect of autophagy in HCC. Inhibition of autophagy at both an early step (by *ATG7* knockdown) and a late step (by chloroquine treatment) sensitized hepatoma cells by converting the autophagic process to an apoptotic process. Of importance are the findings that sorafenib induced autophagy in a xenograft model and that coadministration of chloroquine and sorafenib led to better suppression of xenograft tumor than sorafenib alone. Although further study is needed to elucidate the mechanism(s) involved in autophagy-mediated protection of tumor cells, the induced autophagy might degrade the damaged or harmful cellular proteins and organelles to suppress apoptosis and promote survival of hepatoma cells under sorafenib treatment.

In conclusion, the present study demonstrates both *in vitro* and *in vivo* that sorafenib induces autophagosome formation and upregulates cellular autophagy in tumor cells, which is an adaptive response to this drug, and raises the important possibility that autophagy may be a novel target for cancer treatment with sorafenib therapy.

Acknowledgements

The authors thank David Sabatini's laboratory (Whitehead Institute for Biomedical Research) and Nathanael Gray's laboratory (Dana-Farber Cancer Institute) for providing Torin1. They also thank Bayer HealthCare Pharmaceuticals Inc. (Wayne, NJ) for providing sorafenib.

References

1. Finn RS. Drug therapy: sorafenib. *Hepatology* 2010;51:1843–9.
2. Llovet JM, Ricci S, Mazzaferro V, Hilgard P, Gane E, Blanc JF, de Oliveira AC, Santoro A, Raoul JL, Forner A, Schwartz M, Porta C, et al. Sorafenib in advanced hepatocellular carcinoma. *N Engl J Med* 2008;359:378–90.
3. Cheng AL, Kang YK, Chen Z, Tsao CJ, Qin S, Kim JS, Luo R, Feng J, Ye S, Yang TS, Xu J, Sun Y, et al. Efficacy and safety of sorafenib in patients in the Asia-Pacific region with advanced hepatocellular carcinoma: a phase III randomised, double-blind, placebo-controlled trial. *Lancet Oncol* 2009;10:25–34.
4. Yoshimori T. Autophagy: a regulated bulk degradation process inside cells. *Biochem Biophys Res Commun* 2004;313:453–8.
5. Tsujimoto Y, Shimizu S. Another way to die: autophagic programmed cell death. *Cell Death Differ* 2005;12 (Suppl 2):1528–34.
6. White E, DiPaola RS. The double-edged sword of autophagy modulation in cancer. *Clin Cancer Res* 2009;15:5308–16.
7. Qu X, Yu J, Bhagat G, Furuya N, Hibshoosh H, Troxel A, Rosen J, Eskelinen EL, Mizushima N, Ohsumi Y, Cattoretti G, Levine B. Promotion of tumorigenesis by heterozygous disruption of the beclin 1 autophagy gene. *J Clin Invest* 2003;112: 1809–20.
8. Kondo Y, Kanzawa T, Sawaya R, Kondo S. The role of autophagy in cancer development and response to therapy. *Nat Rev Cancer* 2005;5: 726–34.
9. Ullén A, Farnebo M, Thyrell L, Mahmoudi S, Kharaziha P, Lennartsson L, Grandér D, Panaretakis T, Nilsson S. Sorafenib induces apoptosis and autophagy in prostate cancer cells in vitro. *Int J Oncol* 2010;37:15–20.
10. Park MA, Zhang G, Martin AP, Hamed H, Mitchell C, Hylemon PB, Graf M, Rahmani M, Ryan K, Liu X, Spiegel S, Norris J, et al. Vorinostat and sorafenib increase ER stress, autophagy and apoptosis via ceramide-dependent CD95 and PERK activation. *Cancer Biol Ther* 2008;7:1648–62.
11. Park MA, Reinehr R, Häussinger D, Voelkel-Johnson C, Ogretmen B, Yacoub A, Grant S, Dent P. Sorafenib activates CD95 and promotes autophagy and cell death via Src family kinases in gastrointestinal tumor cells. *Mol Cancer Ther* 2010;9:2220–31.
12. Shimizu S, Takehara T, Hikita H, Kodama T, Miyagi T, Hosui A, Tatsumi T, Ishida H, Noda T, Nagano H, Doki Y, Mori M, et al. The let-7 family of microRNAs inhibits Bcl-xL expression and potentiates sorafenib-induced apoptosis in human hepatocellular carcinoma. *J Hepatol* 2010; 52:698–704.
13. Kimura S, Noda T, Yoshimori T. Dissection of the autophagosome maturation process by a novel reporter protein, tandem fluorescent-tagged LC3. *Autophagy* 2007;3:452–60.
14. Hikita H, Takehara T, Shimizu S, Kodama T, Shigekawa M, Iwase K, Hosui A, Miyagi T, Tatsumi T, Ishida H, Li W, Kanto T, et al. The Bcl-xL inhibitor, ABT-737, efficiently induces apoptosis and suppresses growth of hepatoma cells in combination with sorafenib. *Hepatology* 2010;52:1310–21.
15. Mizushima N, Yoshimori T. How to interpret LC3 immunoblotting. *Autophagy* 2007;3:542–5.
16. Bjørkøy G, Lamark T, Brech A, Outzen H, Perander M, Overvatn A, Stenmark H, Johansen T. p62/SQSTM1 forms protein aggregates degraded by autophagy and has a protective effect on huntingtin-induced cell death. *J Cell Biol* 2005;171:603–14.
17. Sridhar SS, Hedley D, Siu LL. Raf kinase as a target for anticancer therapeutics. *Mol Cancer Ther* 2005;4:677–85.
18. Liu L, Cao Y, Chen C, Zhang X, McNabola A, Wilkie D, Wilhelm S, Lynch M, Carter C. Sorafenib blocks the RAF/MEK/ERK pathway, inhibits tumor angiogenesis, and induces tumor cell apoptosis in hepatocellular carcinoma model PLC/PRF/5. *Cancer Res* 2006;66:11851–8.
19. Blechacz BR, Smoot RL, Bronk SF, Werneburg NW, Sirica AE, Gores GJ. Sorafenib inhibits signal transducer and activator of transcription-3 signaling in cholangiocarcinoma cells by activating the phosphatase shatterproof 2. *Hepatology* 2009;50:1861–70.
20. Díaz-Troya S, Pérez-Pérez ME, Florencio FJ, Crespo JL. The role of TOR in autophagy regulation from yeast to plants and mammals. *Autophagy* 2008;4:851–65.
21. Gingras AC, Gygi SP, Raught B, Polakiewicz RD, Abraham RT, Hoekstra MF, Aebersold R, Sonenberg N. Regulation of 4E-BP1 phosphorylation: a novel two-step mechanism. *Genes Dev* 1999;13:1422–37.
22. Foster KG, Fingar DC. Mammalian target of rapamycin (mTOR): conducting the cellular signaling symphony. *J Biol Chem* 2010;285: 14071–7.
23. Thoreen CC, Kang SA, Chang JW, Liu Q, Zhang J, Gao Y, Reichling LJ, Sim T, Sabatini DM, Gray NS. An ATP-competitive mammalian target of rapamycin inhibitor reveals rapamycin-resistant functions of mTORC1. *J Biol Chem* 2009;284: 8023–32.
24. Kanzawa T, Germano IM, Komata T, Ito H, Kondo Y, Kondo S. Role of autophagy in temozolomide-induced cytotoxicity for malignant glioma cells. *Cell Death Differ* 2004;11:448–57.
25. Paglin S, Hollister T, Delohery T, Hackett N, McMahill M, Sphicas E, Domingo D, Yahalom J. A novel response of cancer cells to radiation involves autophagy and formation of acidic vesicles. *Cancer Res* 2001;61:439–44.
26. Tormo D, Checińska A, Alonso-Curbelo D, Pérez-Guijarro E, Cañón E, Riveiro-Falkenbach E, Calvo TG, Larribere L, Megías D, Mulero F, Piris

MA, Dash R, et al. Targeted activation of innate immunity for therapeutic induction of autophagy and apoptosis in melanoma cells. *Cancer Cell* 2009;16:103–14.
27. Goussetis DJ, Altman JK, Glaser H, McNeer JL, Tallman MS, Platanias LC. Autophagy is a critical mechanism for the induction of the antileukemic effects of arsenic trioxide. *J Biol Chem* 2010;285: 29989–97.
28. Mizushima N, Yoshimori T, Levine B. Methods in mammalian autophagy research. *Cell* 2010;140: 313–26.
29. Seglen PO, Brinchmann MF. Purification of autophagosomes from rat hepatocytes. *Autophagy* 2010;6:542–7.
30. Bampton ET, Goemans CG, Niranjan D, Mizushima N, Tolkovsky AM. The dynamics of autophagy visualized in live cells: from autophagosome formation to fusion with endo/lysosomes. *Autophagy* 2005;1:23–36.
31. Crighton D, Wilkinson S, O'Prey J, Syed N, Smith P, Harrison PR, Gasco M, Garrone O, Crook T, Ryan KM. DRAM, a p53-induced modulator of autophagy, is critical for apoptosis. *Cell* 2006;126:121–34.
32. Amaravadi RK, Yu D, Lum JJ, Bui T, Christophorou MA, Evan GI, Thomas-Tikhonenko A, Thompson CB. Autophagy inhibition enhances therapy-induced apoptosis in a Myc-induced model of lymphoma. *J Clin Invest* 2007;117:326–36.
33. Hussain SP, Schwank J, Staib F, Wang XW, Harris CC. TP53 mutations and hepatocellular carcinoma: insights into the etiology and pathogenesis of liver cancer. *Oncogene* 2007;26: 2166–76.
34. Kisen GO, Tessitore L, Costelli P, Gordon PB, Schwarze PE, Baccino FM, Seglen PO. Reduced autophagic activity in primary rat hepatocellular carcinoma and ascites hepatoma cells. *Carcinogenesis* 1993;14: 2501–5.
35. Ding ZB, Shi YH, Zhou J, Qiu SJ, Xu Y, Dai Z, Shi GM, Wang XY, Ke AW, Wu B, Fan J. Association of autophagy defect with a malignant phenotype and poor prognosis of hepatocellular carcinoma. *Cancer Res* 2008;68: 9167–75.
36. Kiyono K, Suzuki HI, Matsuyama H, Morishita Y, Komuro A, Kano MR, Sugimoto K, Miyazono K. Autophagy is activated by TGF-beta and potentiates TGF-beta-mediated growth inhibition in human hepatocellular carcinoma cells. *Cancer Res* 2009;69:8844–52.

THE JOURNAL OF BIOLOGICAL CHEMISTRY VOL. 287, NO. 26, pp. 22089–22098, June 22, 2012

A Novel Acetylation Cycle of Transcription Co-activator Yes-associated Protein That Is Downstream of Hippo Pathway Is Triggered in Response to S_N2 Alkylating Agents*[S]

Received for publication, December 15, 2011, and in revised form, April 25, 2012 Published, JBC Papers in Press, April 27, 2012, DOI 10.1074/jbc.M111.334714

Shoji Hata[‡], Jun Hirayama[‡], Hiroaki Kajiho[§], Kentaro Nakagawa[¶], Yutaka Hata[¶], Toshiaki Katada[§], Makoto Furutani-Seiki[‖], and Hiroshi Nishina[‡1]

From the [‡]Department of Developmental and Regenerative Biology, Medical Research Institute, Tokyo Medical and Dental University, 1-5-45 Yushima, Bunkyo-ku, Tokyo 113-8510, Japan, the [§]Department of Physiological Chemistry, Graduate School of Pharmaceutical Sciences, University of Tokyo, 7-3-1, Hongo, Bunkyo-ku, Tokyo 113-0033, Japan, the [¶]Department of Medical Biochemistry, Graduate School of Medicine, Tokyo Medical and Dental University, 1-5-45 Yushima, Bunkyo-ku, Tokyo 113-8510, Japan, and the [‖]Centre for Regenerative Medicine, Department of Biology and Biochemistry, University of Bath, Claverton Down, Bath BA2 7AY, United Kingdom

Background: YAP is a target molecule of the Hippo pathway.
Results: YAP acetylation and deacetylation were mediated by CBP/p300 acetyltransferase and SIRT1 deacetylase, respectively.
Conclusion: A YAP acetylation/deacetylation cycle is located downstream of the Hippo pathway.
Significance: The discovery that YAP undergoes an acetylation cycle advances our understanding of YAP functions.

Yes-associated protein (YAP) is a transcriptional co-activator that acts downstream of the Hippo signaling pathway and regulates multiple cellular processes. Although cytoplasmic retention of YAP is known to be mediated by Hippo pathway-dependent phosphorylation, post-translational modifications that regulate YAP in the nucleus remain unclear. Here we report the discovery of a novel cycle of acetylation/deacetylation of nuclear YAP induced in response to S_N2 alkylating agents. We show that after treatment of cells with the S_N2 alkylating agent methyl methanesulfonate, YAP phosphorylation mediated by the Hippo pathway is markedly reduced, leading to nuclear translocation of YAP and its acetylation. This YAP acetylation occurs on specific and highly conserved C-terminal lysine residues and is mediated by the nuclear acetyltransferases CBP (CREB binding protein) and p300. Conversely, the nuclear deacetylase SIRT1 is responsible for YAP deacetylation. Intriguingly, we found that YAP acetylation is induced specifically by S_N2 alkylating agents and not by other DNA-damaging stimuli. These results identify a novel YAP acetylation cycle that occurs in the nucleus downstream of the Hippo pathway. Intriguingly, our findings also indicate that YAP acetylation is involved in responses to a specific type of DNA damage.

The Yes-associated protein (YAP)[2] is a transcriptional co-activator that contributes to the regulation of multiple cellular processes by activating several transcription factors (1). Recently, YAP was shown to play an important role in organ size control and to be inhibited by the Hippo signaling pathway (2–4). Either transgenic overexpression of YAP or knock-out of Hippo pathway genes in mouse liver results in enlargement of this organ and the eventual development of hepatic tumors (5, 6). *In vitro*, YAP overexpression promotes cell proliferation and induces oncogenic transformation by activating TEAD family transcription factors (7, 8). YAP also plays a critical role in maintaining stem cell pluripotency, as knockdown of YAP leads to loss of this property in embryonic stem cells, and YAP overexpression suppresses embryonic stem cell differentiation (9). In certain tumor-derived cell lines exposed to various genotoxic stimuli, YAP promotes apoptosis via the induction of pro-apoptotic genes controlled by the transcription factor p73 (10).

The functions of YAP are regulated by multiple post-translational modifications. Cell-cell contact triggers YAP inactivation via phosphorylation mediated by the Hippo pathway (11). The Hippo pathway component Lats kinase phosphorylates serine 127 (Ser-127) of human YAP (hYAP), promoting its recognition and cytoplasmic retention by 14-3-3 protein. In addition, phosphorylation of hYAP Ser-381 by Lats primes subsequent phosphorylation of hYAP Ser-384 by casein kinase 1, leading to hYAP ubiquitination and degradation (12). On the other hand, the genotoxic agent cisplatin induces promyelocytic leukemia-mediated sumoylation of YAP that prevents its ubiquitination-dependent degradation and stabilizes it (13).

We previously reported that some components of the Hippo pathway are involved in responses to stress stimuli, including

* This work was supported by grants from the Japan Society for the Promotion of Science, the Ministry of Education, Culture, Sports, Science, and Technology of Japan, and the Ministry of Health, Labor, and Welfare of Japan.
[S] This article contains supplemental Table S1 and Figs. S1–S3.
[1] To whom correspondence should be addressed. Tel.: 81-3-5803-4658; Fax: 81-3-5803-5829; E-mail: nishina.dbio@mri.tmd.ac.jp.
[2] The abbreviations used are: YAP, yes-associated protein; hYAP, human YAP; meYAP, medaka; TEAD, TEA domain transcription factor; Lats, large tumor suppressor; MMS, methyl methanesulfonate; CBP, cAMP-response element-binding protein (CREB)-binding protein; p300, E1A-binding protein p300; HDAC, histone deacetylase; NAM, nicotinamide; SIRT, sirtuin; DMS, dimethyl sulfate; MNNG, *N*-methyl-*N*-nitro-*N*-nitrosoguanidine; MNU, *N*-methyl-*N*-nitrosourea; WRN, Werner syndrome helicase; ABH, AlkB homolog; ASCC3, activating signal co-integrator 1 complex subunit 3; Ab, antibody; MTS, 3-(4,5-dimethylthiazol-2-yl)-5-(3-carboxymethoxyphenyl)-2-(4-sulfophenyl)-2H-tetrazolium.

DNA alkylating agents (14, 15). Endogenous and environmental alkylating agents react with specific sites on the nucleic acid bases of DNA or RNA to generate methylated bases that are cytotoxic or mutagenic (16). The alkylating agents generating such bases are classified as either S_N1 or S_N2, depending on their reaction mechanism. The distribution of the methylated products on nucleic acid bases depends not only on the type of alkylating agent but also on whether the nucleic acid targeted is in a single-stranded or double-stranded state (16, 17). S_N2 alkylating agents, but not S_N1 agents, can act on single-stranded DNA and RNA to generate 1-methyladenine and 3-methylcytosine. However, the signal transduction events mediating cellular responses to damage caused by S_N2 alkylating agents are undefined. In this study we show that YAP is involved in specific cellular responses to S_N2 alkylating agents and provide the first evidence that YAP can be post-translationally modified via acetylation in the nucleus.

EXPERIMENTAL PROCEDURES

Plasmids—pCMV-FLAG-hYAP, pCMV-FLAG-TEAD4, pcDNA-VP16-hYAP, and pCS2-meYAP were constructed by inserting PCR-amplified DNA fragments into the indicated vectors. Sequences of PCR primers are listed in supplemental Table S1. The meYAP-13KR, meYAP- 12KR/K, and hYAP-KR mutants were constructed by site-directed mutagenesis. Other plasmids used in this study have been described elsewhere (18).

Reagents—Methyl methanesulfonate (MMS), cisplatin, doxorubicin and *N*-methyl-*N*-nitrosourea (MNU) were purchased from Sigma. Camptothecin, *N*-methyl-*N*-nitro-*N*-nitrosoguanidine (MNNG), and dimethyl sulfate (DMS) were purchased from Tokyo Chemical Industry. H_2O_2 was purchased from Wako Pure Chemical Industries.

Antibodies—Anti-YAP antibody (Ab) has been described previously (19). Polyclonal Abs recognizing Lys-494-acetylated hYAP or Lys-497-acetylated hYAP were generated in rabbits using synthetic peptides corresponding to acetylated human YAP (residues 489–499) (C-VLAATK(Ac)-LDKES) or acetylated human YAP (492–502) (C-ATKLDK(Ac)-ESFLT), respectively. For immunizations, these peptides were conjugated via cysteine to maleimide-activated keyhole limpet hemocyanin. Anti-Ac-YAP (Lys-494) and Anti-Ac-YAP (Lys-497) polyclonal Ab were affinity-purified using the acetylated peptide and the SulfoLink Immobilization Kit for Peptides (Thermo Scientific). Anti-FLAG (M2) Ab was purchased from Sigma; anti-β-actin Ab, anti-CBP (C-20) Ab, and anti-p300 (N-15) Ab were from Santa Cruz; anti-pYAP (Ser-127) Ab and anti-pan-AcK Ab were from Cell Signaling; anti-SIRT1 Ab was from Millipore; anti-HA Ab was from Immunology Consultants Laboratory.

Cell Culture and Transfection—For routine culture, HeLa cells and HEK293T cells were grown in Dulbecco's modified Eagle's medium (Invitrogen) supplemented with 10% fetal bovine serum (normal medium). Transfection with FuGENE HD was performed according to the manufacturer's instructions (Roche Applied Science).

Retroviral Vector Infection—To generate HeLa cells stably expressing hYAP-WT or hYAP-2KR, 293 retroviral packaging cells were transfected with empty retroviral vector or pCLNCX-hYAP constructs. At 48 h post-transfection, retroviral supernatant was supplemented with Polybrene, passed through a 0.22-μm filter, and used to infect HeLa cells. At 36 h post-infection, cells were selected by adding G418 to the culture medium.

RNA Interference—HeLa cells were transfected with siRNA using DharmaFECT 1 (Dharmacon Inc.) according to the manufacturer's instructions. siRNAs specific for CBP (siGENOME SMART pool human CREBBP, M-003477-02), p300 (siGENOME SMART pool human EP300, M-003486-04), or SIRT1 (siGENOME SMART pool human SIRT1, M-003540-01) and control siRNA (siGENOME Non-Targeting siRNA Pool #1, D-001206-13), were obtained from Dharmacon Inc.

MTS Assays—HeLa cells (2×10^3) were plated in a 96-well dish in 100 μl of normal medium/well. For assessment of MMS sensitivity, cells seeded for 24 h were exposed for 1 h to medium containing an increasing concentration (0–3 mM) of MMS. The MMS-containing medium was then replaced with normal medium, and cell survival was assessed using the MTS assay (Promega) at 48 h after MMS exposure.

Immunoprecipitation—Immunoprecipitation and co-immunoprecipitation assays were performed as previously described (18) with some modifications. HeLa cells and HEK293T cells were seeded in 10-cm dishes and treated with DNA-damaging agents or transfected with the appropriate expression vectors as described in the figures. Cells were homogenized in immunoprecipitation buffer (150 mM NaCl, 5 mM EDTA, 15 mM $MgCl_2$, 1% Nonidet P-40, 1 mM DTT, 0.5% deoxycholic acid, and 50 mM Tris-HCl, pH 8.0) or co-immunoprecipitation binding buffer (150 mM NaCl, 1 mM EDTA, 0.5% Nonidet P-40, 1 mM EGTA, 5% glycerol, and 20 mM Tris-HCl, pH 7.4) containing protease inhibitor mixture tablets. Homogenates were clarified by centrifugation for 10 min at 15,000 × *g*. Total protein from the supernatant was incubated for 12 h at 4 °C with the appropriate Abs as described in the figures plus 20 μl of protein G-agarose beads (GE Healthcare). The beads were washed 3 times with immunoprecipitation buffer or co-immunoprecipitation wash buffer containing 1% Nonidet P-40 and boiled in SDS sample buffer. The supernatant was fractionated by SDS-PAGE and analyzed by standard immunoblotting.

Immunofluorescence—HeLa cells were cultured on a glass coverslip and fixed with 4% paraformaldehyde in PBS at room temperature. After treatment with 0.2% Triton X-100 in PBS, the cells were incubated with blocking solution (5% bovine serum albumin in TBS) before incubation with primary Abs for 1 h at room temperature. Cells were washed with PBS and incubated for 1 h with Alexa 488- or 546-conjugated secondary Abs. After PBS washes, coverslips were mounted and viewed on a Carl Zeiss confocal microscope equipped with LSM510 software.

Luciferase Reporter Assay—HEK293T cells or HeLa cells were plated in 12-well plates at 1.5×10^5 cells per well and incubated overnight. Cells were transfected the next day with 20 ng of firefly luciferase reporter plasmid (p5xUAS-c-fos-promoter-Luc or 8xGT-IIC-δ51LucII) and 5 ng of sea pansy luciferase reporter plasmid (pRL-CMV; from Promega) plus 40 ng of total of expression plasmids (as indicated in the figures). The pcDNA vector was added as needed to make up the total

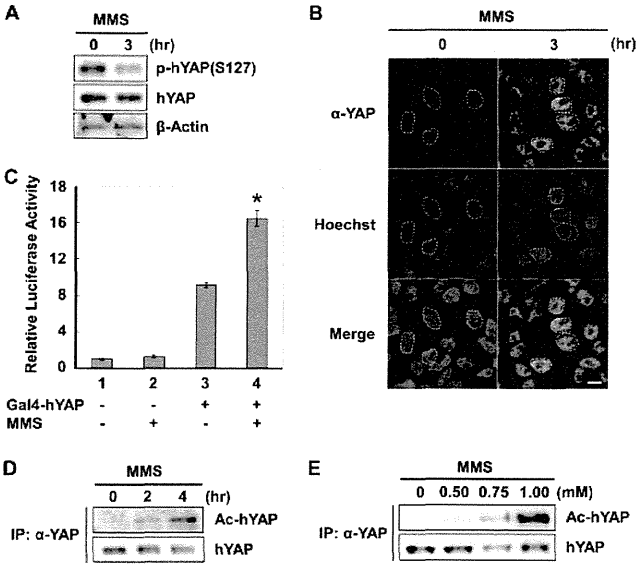

FIGURE 1. **hYAP translocates to the nucleus and is acetylated upon MMS treatment.** *A* and *B*, HeLa cells were treated with 1 mM MMS for 0 or 3 h. *A*, cell lysates were immunoblotted to detect total and Ser-127-phosphorylated hYAP. β-Actin was the loading control. *B*, *top*, shown is immunofluorescence visualization of endogenous hYAP localization by staining with anti-YAP Ab (*green*). *Middle*, shown is Hoechst staining of nuclei (*blue*). Selected nuclei are indicated by a *dashed outline*. *Scale bar*, 10 μm. *C*, HeLa cells were transfected with the Upstream Activation Sequence (UAS)-luciferase reporter construct with or without Gal4-hYAP and treated (or not) with 1 mM MMS for 3 h as indicated. The level of hYAP-dependent transcription was expressed as relative luciferase activity. Values shown are the mean ± S.D. ($n = 3$/group). *, $p < 0.01$, compared with *lane 3*. *D* and *E*, HeLa cells were treated with 1 mM MMS for the indicated times (*D*) or with the indicated concentrations of MMS for 4 h (*E*). Endogenous hYAP was immunoprecipitated (*IP*) and acetylated hYAP (*Ac-hYAP*) was detected by immunoblotting with anti-pan-AcK Ab. For all figures, results shown are representative of at least three independent trials.

amount of expression plasmid DNA. At 24 h post-transfection, luciferase activities were assayed using the dual luciferase reporter assay system (Promega) according to the manufacturer's instructions. Firefly and sea pansy luciferase activities were quantified using a luminometer, with firefly luciferase activity normalized for transfection efficiency based on sea pansy luciferase activity.

Statistical Analyses—The significance of differences was determined using two-tailed Student's *t* test. Differences were considered statistically significant for $p < 0.05$. All experiments were performed three times with similar results.

RESULTS

MMS Treatment Induces Nuclear Translocation and Acetylation of hYAP—To investigate the regulation of hYAP in response to DNA damage, we treated HeLa cells with the S_N2 alkylating agent MMS and examined the phosphorylation status of hYAP Ser-127. We found that hYAP Ser-127 phosphorylation was markedly reduced upon MMS treatment (Fig. 1*A*). Consistent with previous evidence showing that the inhibition of hYAP Ser-127 phosphorylation causes hYAP to translocate to the nucleus, MMS treatment also induced hYAP nuclear translocation (Fig. 1*B*). To assess the effect of MMS treatment on hYAP-dependent transcription, we utilized a reporter system consisting of the UAS-luciferase reporter and the Gal4 DNA binding domain fused to hYAP (Gal4-hYAP) (1). In this assay, exposure to MMS significantly enhanced Gal4-hYAP-dependent luciferase reporter activity (Fig. 1*C*), indicating that hYAP-dependent transcription is up-regulated upon MMS treatment.

To investigate whether hYAP underwent a qualitative change in response to MMS treatment, we carried out a screen to identify post-translational modifications of hYAP. We used anti-YAP Ab to immunoprecipitate endogenous hYAP from lysates of MMS-treated HeLa cells and performed immunoblotting using several Abs that recognize specific post-translational modifications. As shown in Fig. 1*D*, we found that the endogenous hYAP present in MMS-treated HeLa cells could be detected by anti-pan-AcK Ab, which specifically recognizes acetylated lysine residues. Moreover, this hYAP acetylation was induced in a dose-dependent manner (Fig. 1*E*). These results clearly show that endogenous hYAP is acetylated in response to MMS treatment.

hYAP Acetylation Is Mediated by CBP/p300—The above data prompted us to identify the histone acetyltransferases responsible for hYAP acetylation. Because MMS treatment induced both the nuclear translocation and acetylation of hYAP, we focused on the abilities of CBP, p300, and CLOCK, which are histone acetyltransferases localized in the nucleus, to acetylate hYAP (18, 20). We found that co-expression in HEK293T cells of HA-tagged CBP or HA-p300 with FLAG-tagged hYAP significantly increased hYAP acetylation (Fig. 2*A*). In contrast, hYAP acetylation was not induced by CLOCK under conditions in which the well established CLOCK target BMAL1b was acetylated (Fig. 2*B*). Thus, hYAP acetylation is induced specifically by the closely related histone acetyltransferases CBP and p300.

To determine whether hYAP physically interacts with CBP/p300, we first performed co-immunoprecipitation assays which revealed that HA-CBP co-immunoprecipitated with FLAG-hYAP but not with FLAG-TEAD4 (Fig. 2*C*). To confirm this result, we performed mammalian two-hybrid assays (21) in which hYAP fused to the VP16 transactivation domain (VP16-hYAP) was co-expressed in HEK293T cells with CBP or BMAL1b fused to the GAL4 DNA binding domain. Only when VP16-hYAP was co-expressed with GAL4-CBP and not with Gal4-BMAL1b was luciferase reporter activity significantly increased (Fig. 2*D*). These results indicate that hYAP physically interacts with CBP.

To investigate the effect of MMS treatment on CBP/p300-induced hYAP acetylation, we treated HEK293T cells expressing HA-CBP or HA-p300 with MMS. Notably, acetylation of endogenous hYAP was synergistically enhanced by a combination of CBP/p300 expression and MMS treatment (Fig. 2*E*). These data imply that CBP/p300 serves as the histone acetyltransferase that acetylates hYAP in response to MMS treatment.

CBP-mediated Acetylation of YAP Targets Its C-terminal Lysine Residues—To identify the hYAP lysines targeted by CBP-mediated acetylation, we first compared the predicted amino acid sequences of human YAP, mouse YAP, and the YAP (meYAP) present in the small fish medaka. This analysis showed that there are 13 lysines shared by hYAP and meYAP (Fig. 3*A* and supplemental Fig. S1) and that meYAP contains no

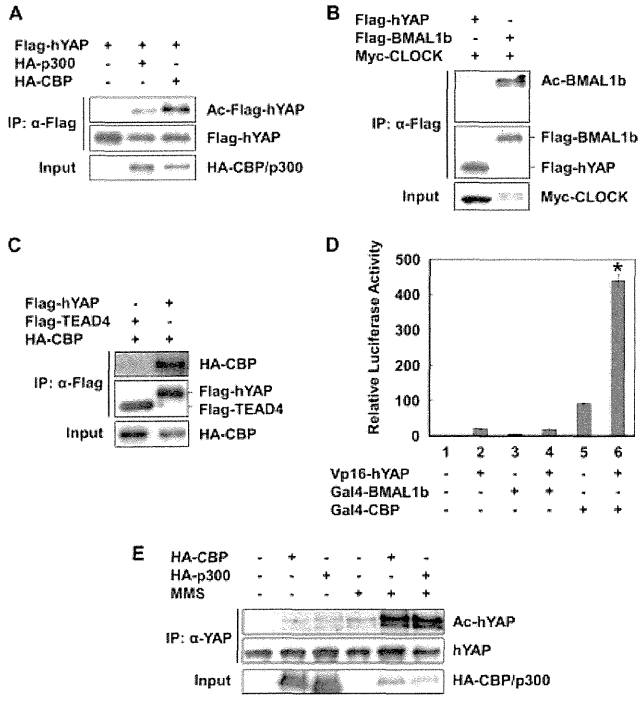

FIGURE 2. **CBP/p300 mediates hYAP acetylation.** *A*, FLAG-hYAP was coexpressed with HA-p300 or HA-CBP in HEK293T cells. Immunoprecipitated (*IP*) FLAG-hYAP was immunoblotted to detect acetylated hYAP. *B*, HEK293T cells were transfected with the indicated plasmids. FLAG-hYAP and FLAG-BMAL1b were immunoprecipitated and immunoblotted to detect the indicated acetylated proteins. *C*, HEK293T cells were transfected with indicated plasmids. FLAG-hYAP and FLAG-TEAD4 were immunoprecipitated and immunoblotted to detect HA-CBP. *D*, HEK293T cells were cotransfected with the luciferase reporter construct and the indicated plasmids. Results are the relative luciferase activity analyzed as for Fig. 1*C*. Values shown are the mean ± S.D. (n = 3/group). *, $p < 0.01$, compared with *lane 5*. *E*, HEK293T cells transfected with HA-CBP, or HA-p300 were treated with 1 mM MMS for 3 h, as indicated. Endogenous hYAP was immunoprecipitated, and acetylated hYAP was detected by immunoblotting.

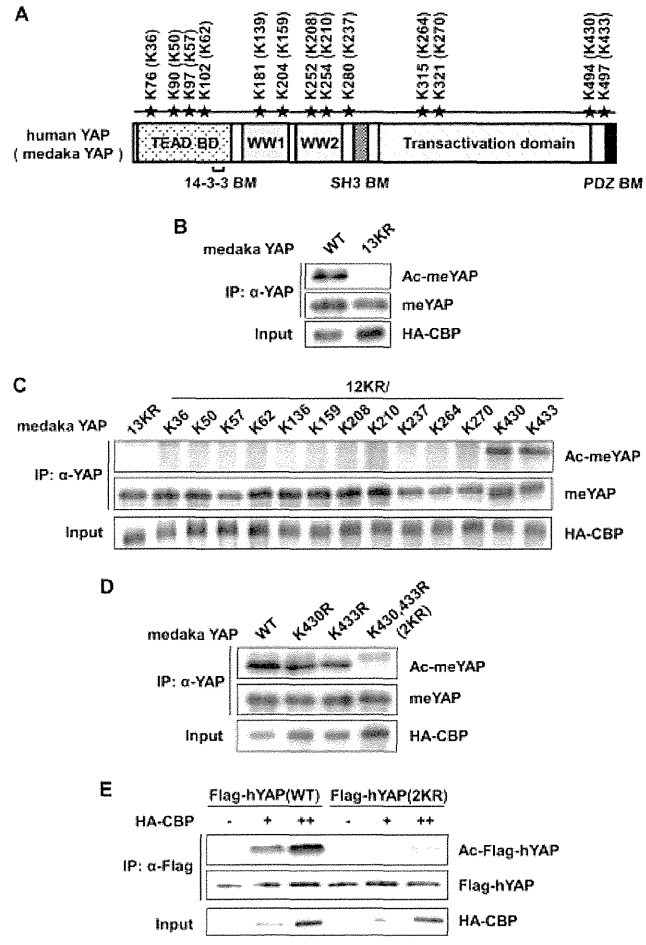

FIGURE 3. **CBP-mediated acetylation of YAP targets conserved C-terminal lysines.** *A*, a schematic representation of the human and medaka (in *parentheses*) YAP protein shows domains TEAD binding domain (*BD*), 14-3-3 binding motif (*BM*), WW1/2 domains, SH3 BM, transactivation domain, and PDZ BM. The positions of lysine residues (*black stars*) in both species are indicated. *B–E*, HEK293T cells were cotransfected with HA-CBP plus the indicated medaka or human YAP constructs in which all 13 conserved lysine residues were mutated to arginine (13KR), or 12 lysines were mutated to arginine (12KR), and the indicated lysine was not mutated. Immunoprecipitated (*IP*) meYAP (*B–D*) or FLAG-hYAP (*E*) was immunoblotted with anti-pan-AcK Ab to detect acetylated hYAP.

additional lysines. This evolutionary conservation of critical lysine residues allowed us to utilize meYAP protein for the identification of common hYAP acetylation sites.

To determine precisely which YAP lysines are acetylated by CBP/300, we generated a meYAP-13KR mutant in which all lysine residues were replaced by arginine residues. As expected, CBP-mediated acetylation of meYAP-13KR was completely abolished (Fig. 3*B*). We then restored individual lysines one at a time in meYAP- 13KR to generate a series of meYAP-12KR/K mutants in which each retained a single, different lysine residue. Strikingly, restoration of Lys-430 or Lys-433 allowed resumption of CBP-mediated acetylation of meYAP-13KR (Fig. 3*C*). Consistent with this result, a meYAP-2KR mutant in which Lys-430 and Lys-433 were replaced with arginines exhibited dramatically reduced CBP-mediated acetylation compared with wild type (WT) meYAP (Fig. 3*D*). Finally, we determined whether hYAP is also acetylated at its conserved C-terminal lysines. Analogous to our results with meYAP, mutation of the C-terminal lysines 494 and 497 in FLAG-hYAP significantly reduced its CBP-mediated acetylation (Fig. 3*E*). Taken together, these data demonstrate that evolutionarily conserved lysine residues at the C terminus of YAP are targets for CBP-mediated acetylation.

CBP/p300 Mediates Lys-494 Acetylation of hYAP upon MMS Treatment—To investigate site-specific hYAP acetylation at the endogenous level, we prepared polyclonal Abs that specifically recognized the hYAP protein acetylated at Lys-494 or Lys-497. We first confirmed that these Abs detected exogenously expressed WT hYAP in the presence of HA-CBP expression but did not recognize mutant hYAP proteins bearing altered acetylation sites (Fig. 4*A*). Next, we used these Abs to confirm that both Lys-494 and Lys-497 of endogenous hYAP are acetylated upon MMS treatment (Fig. 4*B*). Immunofluorescence analysis using anti-Ac-YAP (Lys-494) Ab showed that exogenously expressed FLAG-hYAP-WT, but not FLAG-hYAP-2KR, was acetylated after MMS treatment (Fig. 4*C*). Because the anti-Ac-YAP (Lys-497) Ab was unsuitable for immunofluorescence analysis (data not shown), we utilized the anti-AcYAP (Lys-494) Ab for subsequent studies.

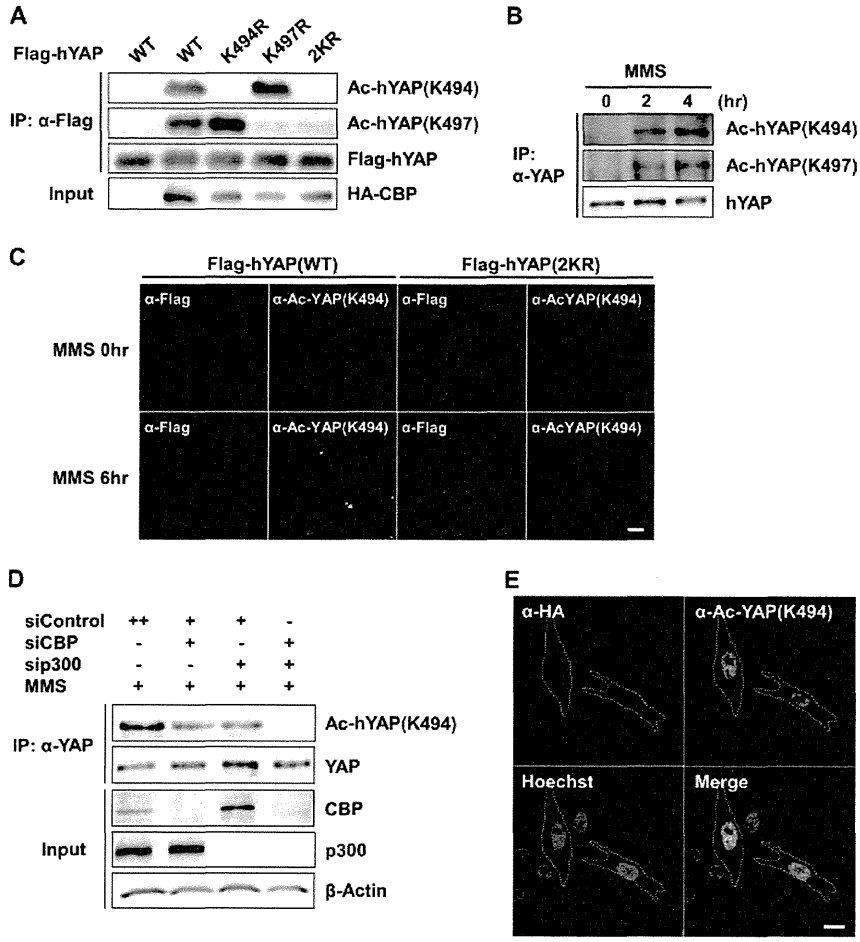

FIGURE 4. **CBP and p300 mediate Lys-494 acetylation of hYAP upon MMS treatment.** *A*, HEK293T cells were cotransfected with HA-CBP and the indicated WT or mutant hYAP constructs. Immunoprecipitated (*IP*) FLAG-hYAP was immunoblotted with anti-Ac-YAP (Lys-494) or anti-Ac-YAP (Lys-497) Ab. *B*, HeLa cells were treated with 1 mM MMS for the indicated times. Endogenous hYAP was immunoprecipitated and immunoblotted to detect total, Lys-494-acetylated, and Lys-497-acetylated hYAP. *C*, HeLa cells transfected with FLAG-hYAP (WT), or FLAG-hYAP (2KR) were treated with 1 mM MMS for 0 or 6 h. Total FLAG-hYAP and Lys-494-acetylated hYAP were visualized by immunofluorescence staining with anti-FLAG (*red*) or anti-Ac-YAP (Lys-494) (*green*) Ab. *Scale bar*, 25 μm. *D*, HeLa cells were transfected with the indicated siRNAs. After 72 h, cells were treated with 1 mM MMS for 6 h. Cell lysates were immunoblotted to detect the indicated proteins. *E*, HeLa cells were transfected with HA-CBP, and the localization of endogenous Lys-494-acetylated hYAP was visualized by immunofluorescence staining with anti-Ac-YAP (Lys-494) Ab (*green*). Cells expressing HA-CBP were visualized by immunostaining with anti-HA Ab (*red*) and are outlined with *dashed lines*. Nuclei were visualized by Hoechst staining (*blue*). *Scale bar*, 10 μm.

To investigate whether MMS-induced acetylation of hYAP Lys-494 is mediated by CBP/p300, we down-regulated CBP and/or p300 expression in HeLa cells using RNA interference (RNAi). Double knockdown of CBP and p300 completely reduced endogenous hYAP Lys-494 acetylation upon MMS treatment (Fig. 4*D*), indicating that MMS-induced acetylation of hYAP at Lys-494 can indeed be mediated by either CBP or p300. Because CBP and p300 are both nuclear proteins, we speculated that hYAP Lys-494 acetylation occurs in the nucleus. To determine the subcellular localization of endogenous Lys-494-acetylated hYAP, we performed an immunofluorescence analysis of HeLa cells transfected with HA-CBP. Endogenous Lys-494-acetylated hYAP was detected mainly in the nuclei of these cells (Fig. 4*E*). Taken together, these results indicate that the acetylation of hYAP Lys-494 that is induced by MMS is mediated by CBP and/or p300 and takes place in the nucleus.

SIRT1 Is Responsible for Deacetylation of hYAP Lys-494—Lysine acetylation is a reversible protein modification, and deacetylation of acetylated lysine is catalyzed by histone deacetylases (HDAC). HDACs are grouped into four classes according to phylogenetic analysis and sequence homology (22). To identify the HDACs responsible for deacetylation of hYAP Lys-494, we utilized class-specific HDAC inhibitors. When we treated HeLa cells with nicotinamide (NAM), an inhibitor of class III HDACs, MMS-induced acetylation of endogenous hYAP Lys-494 was markedly increased (Fig. 5*A*). In contrast, treatment with trichostatin A, an inhibitor of class I and II HDACs, had no effect on hYAP Lys-494 acetylation. Consistent with these results, CBP-mediated hYAP Lys-494 acetylation was also enhanced by NAM treatment but not by trichostatin A (Fig. 5*B*). Intriguingly, even in the absence of MMS, acetylation of endogenous hYAP Lys-494 was induced in a time-dependent manner after NAM treatment (Fig. 5*C*).

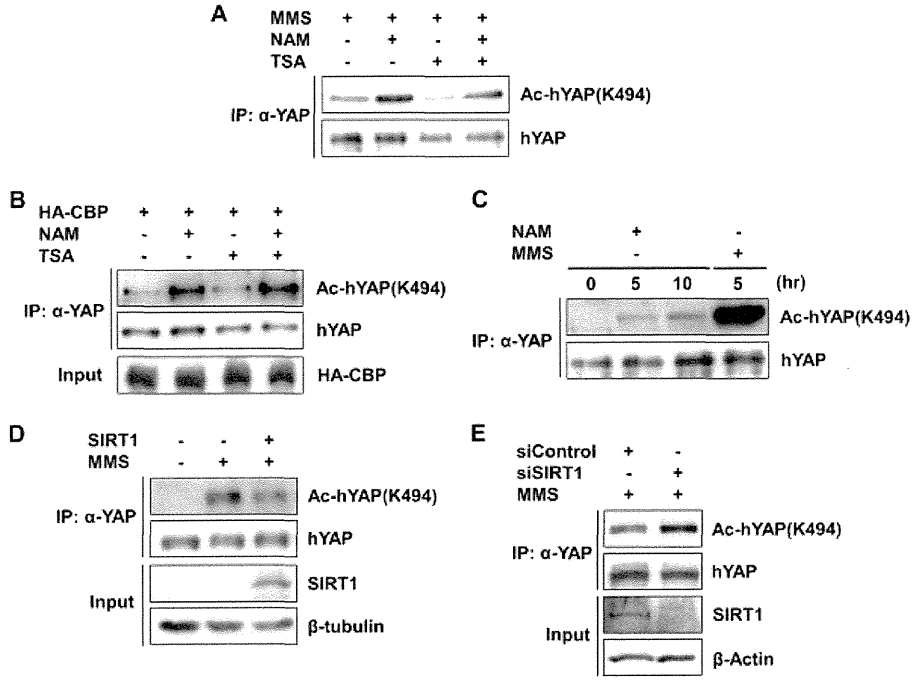

FIGURE 5. **SIRT1 induces deacetylation of Lys-494-acetylated hYAP.** *A*, HeLa cells were treated for 6 h with 1 mM MMS with or without 10 mM NAM or 1 μM trichostatin A (*TSA*) as indicated. Endogenous hYAP was immunoprecipitated (*IP*), and Lys-494-acetylated hYAP was detected by immunoblotting. *B*, HEK293T cells transfected with HA-CBP were treated for 6 h with 10 mM NAM and/or 1 μM trichostatin A as indicated. Endogenous hYAP was immunoprecipitated, and the indicated proteins were detected by immunoblotting. *C*, HeLa cells were treated with 10 mM NAM or 1 mM MMS for the indicated times, and lysates were analyzed as for *A*. *D*, HeLa cells transfected with SIRT1 were treated (or not) with 1 mM MMS for 6 h as indicated. Endogenous hYAP was immunoprecipitated, and the indicated proteins were detected by immunoblotting. β-Tubulin was the loading control. *E*, HeLa cells were transfected with the indicated siRNAs. After 72 h, cells were treated with 1 mM MMS for 6 h. Cell lysates were analyzed as for *D*.

These results suggest that the acetylation-deacetylation cycle involving hYAP Lys-494 operates regardless of extrinsic DNA damage and that the deacetylation of this residue is catalyzed by a class III HDAC.

The class III HDAC Sirtuin 1 (SIRT1) is reportedly transcriptionally up-regulated by MMS treatment and involved in responses to this agent (23). These observations prompted us to test whether SIRT1 might mediate hYAP Lys-494 deacetylation. Exogenous expression of SIRT1 in HeLa cells significantly decreased MMS-induced acetylation of hYAP Lys-494 (Fig. 5*D*). Consistent with this finding, knockdown of SIRT1 enhanced MMS-induced hYAP Lys-494 acetylation (Fig. 5*E*). Thus, SIRT1 is at least one of the class III HDACs responsible for deacetylating Lys-494-acetylated hYAP.

S_N2 Alkylating Agents Specifically Induce Both Acetylation and Ser-127 Dephosphorylation of hYAP—YAP has previously been shown to be involved in cellular responses to a variety of DNA-damaging agents (10, 24, 25). Therefore, we investigated the effects of several DNA-damaging agents other than MMS on both hYAP Ser-127 phosphorylation and hYAP acetylation. Because cisplatin treatment induces nuclear translocation of hYAP (10) and H_2O_2 treatment activates the Hippo pathway (6, 19), we treated HeLa cells with cisplatin or H_2O_2 and examined hYAP Ser-127 phosphorylation and hYAP acetylation. Intriguingly, hYAP Ser-127 phosphorylation was down-regulated in a dose-dependent manner after cisplatin treatment but up-regulated in a dose-dependent manner upon H_2O_2 treatment (Fig. 6*A*). However, in contrast to MMS, neither cisplatin nor H_2O_2 induced the acetylation of endogenous hYAP (Fig. 6*B*). Nor was hYAP acetylation induced in HeLa cells by treatment with other DNA-damaging agents, including camptothecin or doxorubicin (supplemental Fig. S2). These data indicate that hYAP regulation by the Hippo pathway is differentially altered by different types of DNA damage and that hYAP acetylation may be a regulatory event specific to DNA alkylating agents such as MMS.

As mentioned above, alkylating agents are classified as being of either the S_N1 or S_N2 type depending on their reaction mechanism (16). Because MMS is an S_N2 alkylating agent, we first investigated whether another S_N2 agent could induce hYAP acetylation by treating HeLa cells with DMS. As expected, DMS treatment also resulted in a dose-dependent decrease in hYAP Ser-127 phosphorylation (Fig. 6*C*) and a dose-dependent increase in hYAP acetylation (Fig. 6*D*). We then treated HeLa cells with either of two S_N1 alkylating agents, MNNG or MNU. Phosphorylation of hYAP Ser-127 was reduced by MNNG treatment but not altered upon MNU exposure (Fig. 6*E*). Intriguingly, neither MNNG nor MNU could induce hYAP acetylation (Fig. 6*F*). These results indicate that S_N2 alkylating agents specifically induce two relevant events, 1) the release of hYAP from Hippo pathway-mediated cytoplasmic retention and 2) the up-regulation of CBP/p300-mediated hYAP acetylation in the nucleus.

hYAP Acetylation Affects Cellular Responses to MMS Treatment—YAP is known to be an important regulator of cell viability (2). To put our results in a biological context, we inves-

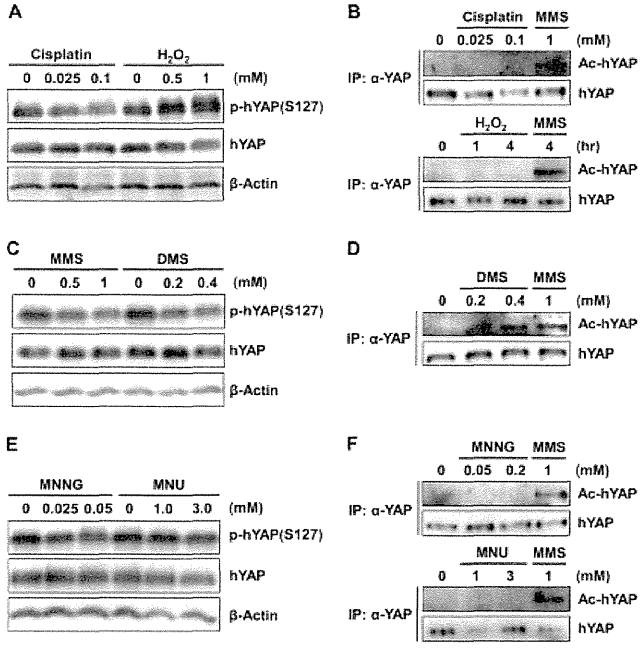

FIGURE 6. **DNA-damaging agents have diverse effects on hYAP Ser-127 phosphorylation and hYAP acetylation.** *A*, HeLa cells were treated with the indicated concentrations of cisplatin or H_2O_2 for 6 or 3 h, respectively. Total and Ser-127-phosphorylated hYAP were detected by immunoblotting. *B*, HeLa cells were treated with the indicated concentrations of cisplatin for 12 h or 1 mM MMS for 4 h (*top*) or 1 mM H_2O_2 for the indicated times or 1 mM MMS for 4 h (*bottom*). Endogenous hYAP was immunoprecipitated (*IP*), and acetylated hYAP was detected by immunoblotting with anti-pan-AcK Ab. *C*, HeLa cells were treated with the indicated concentrations of MMS or DMS for 3 h. Cell lysates were analyzed as for *A*. *D*, HeLa cells were treated with the indicated concentrations of DMS or MMS for 4 h. Cell lysates were analyzed as for *B*. *E*, HeLa cells were treated with the indicated concentrations of MNNG or MNU for 3 h. Cell lysates were analyzed as for *A*. *F*, HeLa cells were treated for 4 h with the indicated concentrations of MNNG or MMS (*top*) or MNU or MMS (*bottom*). Cell lysates were analyzed as for *B*.

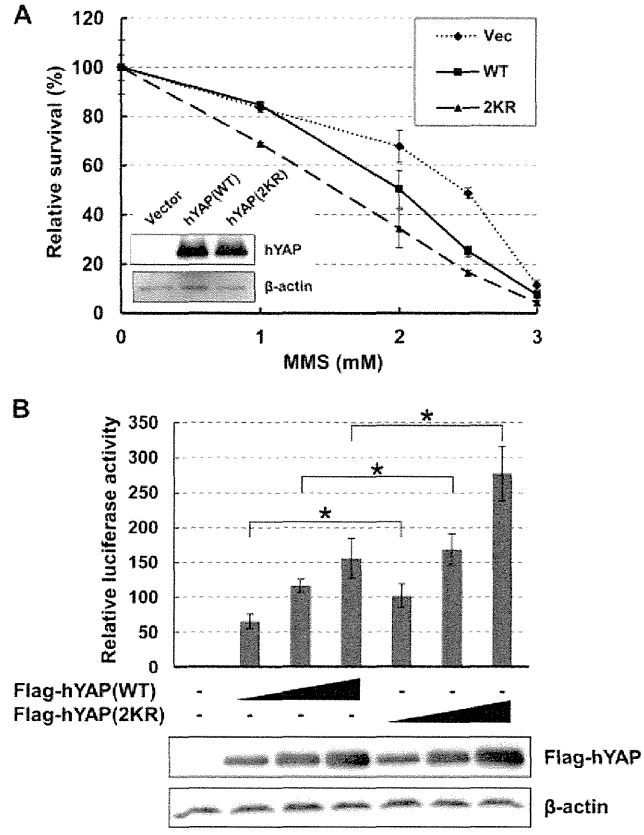

FIGURE 7. **Expression of the acetylation-resistant hYAP-2KR protein alters cellular responses to MMS treatment.** *A*, HeLa cells stably expressing hYAP-WT or hYAP-2KR were exposed to the indicated concentrations of MMS for 1 h, and survival was assessed 48 h later by MTS assay. Values shown are the mean ± S.D. (n = 3/group). *Inset*, shown is an immunoblot to confirm hYAP expression in the above cells before MMS treatment. *B*, 293T cells were co-transfected with 8xGT-IIC-δ51LucII and increasing amounts of the indicated plasmids and treated with 1 mM MMS for 3 h. Luciferase activity was measured and normalized to cotransfected renilla luciferase activity. Values shown are the mean ± S.D. (n = 3/group). *, $p < 0.01$. The expression levels of transfected FLAG-hYAP were detected by immunoblotting.

tigated whether hYAP acetylation influenced cellular responses to MMS treatment. We established HeLa cells stably expressing hYAP-WT or hYAP-2KR by retroviral vector infection and exposed them to increasing concentrations of MMS. Cell survival was assessed using a tetrazolium-based colorimetric viability assay (MTS). Interestingly, expression of hYAP-2KR significantly decreased cell survival compared with hYAP-WT expression (Fig. 7*A*), indicating that hYAP acetylation affects the sensitivity of HeLa cells to MMS treatment.

Next, we examined whether hYAP acetylation is important for its nuclear translocation after MMS exposure. As shown in supplemental Fig. S3, both the FLAG-hYAP-WT and FLAG-hYAP-2KR proteins accumulated in the nuclei of MMS-treated HeLa cells. Thus, the MMS-induced nuclear localization of hYAP is not affected by hYAP acetylation.

To investigate the physiological significance of hYAP acetylation in the nucleus, we co-transfected 293T cells with a synthetic YAP responsive luciferase reporter (8xGT-IIC-δ51LucII) (26) and FLAG-hYAP-WT or FLAG-hYAP-2KR. These cells were then exposed to MMS, and luciferase activity was measured. As shown in Fig. 7*B*, cells expressing FLAG-hYAP-2KR exhibited significantly higher luciferase activity than cells expressing FLAG-hYAP-WT, indicating that the transcriptional coactivator activity of hYAP is regulated by its acetylation. Taken together, these data suggest that cell fate decisions made in response to MMS-induced DNA damage may be governed by hYAP-dependent gene induction that is regulated by hYAP acetylation.

DISCUSSION

In this study we present evidence for a novel YAP acetylation cycle downstream of Hippo signaling. We have shown that MMS treatment causes a reduction in hYAP Ser-127 phosphorylation mediated by the Hippo pathway, promoting the nuclear translocation of this transcriptional co-activator. Through a screen for post-translational modifications of hYAP, we have demonstrated that hYAP is acetylated at the endogenous level upon MMS treatment. This MMS-induced acetylation of YAP is mediated by the nuclear acetyltransferases CBP and p300, occurs on conserved C-terminal lysine residues, and can be reversed by SIRT1. Importantly, this acetylation-deacetylation cycle of hYAP is triggered specifically in response to S_N2 alkylating agents and not by other types of DNA-damaging stimuli. A schematic model summarizing our findings appears in Fig. 8.

YAP Acetylation Cycle Downstream of the Hippo Pathway

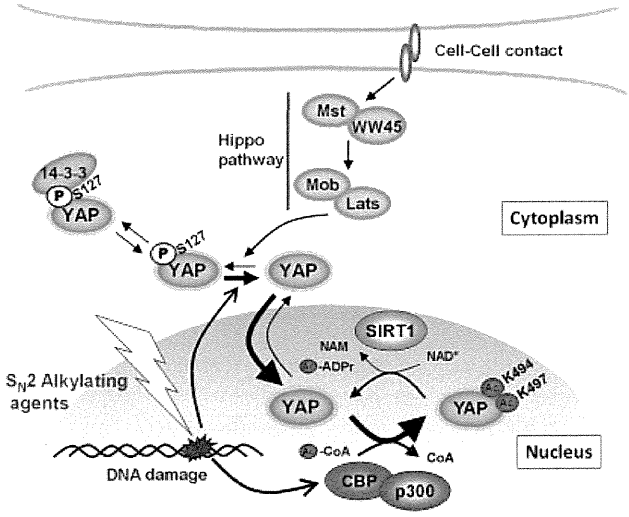

FIGURE 8. **A proposed model for hYAP regulation in response to S_N2 alkylating agents.** Cell-cell contact triggers Hippo pathway signaling that up-regulates Ser-127 phosphorylation of hYAP and thus its cytoplasmic retention via binding to 14-3-3 protein. S_N2 alkylating agents damage DNA, leading to a reduction in Ser-127 phosphorylation of hYAP. Non-phosphorylated hYAP is released from the cytoplasmic 14-3-3 complex and translocates into the nucleus. Within the nucleus, CBP and/or p300 activated by S_N2 alkylating agent-mediated DNA damage induce hYAP acetylation at Lys-494 and Lys-497. Concurrently, deacetylation of these residues is mediated by SIRT1. Thus, tight regulation governs the state of hYAP acetylation induced in response to S_N2 alkylating agents.

Our results have revealed that Lys-494 and Lys-497 of hYAP are targets for CBP-mediated acetylation. In previous reports, CBP and p300 were shown to directly acetylate a variety of proteins at a consensus motif ($KX_{1-2}(X/K)K$) (27–30). Notably, hYAP contains this consensus motif (^{494}KLDK^{497}), and the hYAP acetylation sites identified in our experiments are consistent with the positions of two of the lysine residues present in this motif. Interestingly, although the acetylation consensus motif is conserved among vertebrate YAPs (human, mouse, and medaka), it is not found in either Yki (yorkie), the *Drosophila* homologue of YAP, or in TAZ (transcriptional coactivator with PDZ-binding motif), a vertebrate paralogue of YAP (4). Thus, the CBP/p300-dependent acetylation we observe appears to be a modification specific to vertebrate YAP.

A number of studies have reported that CBP/p300-mediated acetylation of several proteins is important for cellular responses to DNA damage. For example, the Werner syndrome helicase (WRN) helps to promote the survival of cells with damaged DNA. CBP-mediated acetylation of WRN triggered by DNA damage inhibits the ubiquitination-dependent degradation of this helicase and thus increases its stability (31). Similarly, DNA damage induces p300 to acetylate and stabilize Nijmegen breakage syndrome 1, which plays a crucial role in homologous recombination repair (32). The acetylation of proteins involved in DNA damage responses is often countered by SIRT1-mediated deacetylation (33), and acetylated WRN and Nijmegen breakage syndrome 1 are both substrates of SIRT1 (34, 35). The importance of such acetylation-deacetylation cycles has been highlighted by the significant increase in chromosomal aberrations identified in SIRT1-deficient cells (36). Our study has revealed that hYAP also undergoes reversible acetylation and deacetylation mediated by CBP/p300 and SIRT1, respectively. More importantly, our results indicate that acetylation of hYAP influences both its transcriptional co-activator activity and the sensitivity of hYAP-expressing cells to MMS-induced DNA damage.

Different genotoxic agents induce different types of DNA damage, and these lesions trigger lesion-specific DNA repair mechanisms. YAP has previously been shown to participate in responses to DNA-damaging agents such as cisplatin, adriamycin, ultraviolet radiation, and ionizing radiation (10, 24, 25), but the lesion-specific aspects of YAP regulation were not defined in these studies. In this report we have demonstrated that hYAP Ser-127 phosphorylation mediated by the Hippo pathway is differentially altered depending on the type of DNA-damaging agent encountered. Our data show that DNA-damaging stimuli can be classified into at least three groups based on their effects on the subcellular localization and post-translational modification of hYAP; Group I, Hippo pathway-mediated hYAP Ser-127 phosphorylation is up-regulated and hYAP remains in the cytoplasm; Group II, hYAP Ser-127 phosphorylation is down-regulated, and hYAP undergoes nuclear translocation but is not acetylated; Group III, hYAP Ser-127 phosphorylation is down-regulated, and hYAP undergoes both nuclear translocation and acetylation. In line with previous reports (6, 19), we have demonstrated that H_2O_2 treatment of HeLa cells results in up-regulated hYAP Ser-127 phosphorylation (Group I), whereas cisplatin treatment down-regulated Ser-127 phosphorylation but had no effect on acetylation (Group II). Treatment of HeLa cells with MNNG had a similar effect, placing this agent in Group II. The most interesting aspect of our work is the identification of the new Group III, represented solely by S_N2 alkylating agents, which both down-regulate Ser-127 hYAP phosphorylation and induce hYAP acetylation.

Our findings indicate that mere nuclear accumulation of hYAP is not enough to induce its acetylation, and another factor(s) must play an important role in this reaction. Along these lines, we demonstrated that CBP and p300 are key mediators of MMS-induced hYAP acetylation, implying that up-regulation of CBP/p300 activity may be the additional factor contributing to hYAP acetylation. Collectively, our data imply that the specific cellular response to DNA lesions caused by S_N2 alkylating agents involves the coupling of hYAP nuclear translocation induced by Ser-127 dephosphorylation with the activation of CBP/p300-mediated acetylation.

S_N2 alkylating agents, but not S_N1 agents, generate 1-methyladenine and 3-methylcytosine residues in single-stranded DNA and RNA. These cytotoxic lesions are known to be repaired by AlkB family dioxygenases (16). In mammalian cells, AlkB homolog 2 (ABH2) removes 1-methyladenine lesions in genomic DNA and thus is critical for cellular defense against MMS treatment (17). In addition, ABH3 collaborates with ASCC3 helicase to remove 3-methylcytosine lesions in certain tumor-derived cell lines (37). However, the mechanisms regulating ABH2 and ABH3 in response to S_N2 alkylating agents remain largely unknown. Intriguingly, 1-methyladenine accumulates in aging ABH2-deficient mice (17) and 3-methylcytosine accumulates in ABH3 or ASCC3 knockdown cells (37), clearly showing that such cytotoxic methylation events occur endogenously. Rele-

vant in this context is the fact that *S*-adenosylmethionine, which is the methyl group donor in the majority of enzymatic methylation events, can act as an endogenous S_N2 alkylating agent and generates the same methylated adducts on DNA as MMS (38). We found that even in the absence of MMS exposure, acetylation of endogenous hYAP was observed after treatment with the class III HDAC inhibitor NAM. Thus, the hYAP acetylation cycle downstream of the Hippo pathway may occur in response to endogenous single-strand DNA/RNA alkylation events induced by physiological S_N2 alkylating agents. It is, therefore, tempting to speculate that Hippo-YAP signaling may be involved in the intrinsic AlkB-mediated DNA repair pathway.

Acknowledgment—We are grateful to Dr. Hiroshi Sasaki (Kumamoto University) for providing the 8xGT-IIC-δ51LucII plasmid.

REFERENCES

1. Yagi, R., Chen, L. F., Shigesada, K., Murakami, Y., and Ito, Y. (1999) A WW domain-containing yes-associated protein (YAP) is a novel transcriptional co-activator. *EMBO J.* **18,** 2551–2562
2. Halder, G., and Johnson, R. L. (2011) Hippo signaling. Growth control and beyond. *Development* **138,** 9–22
3. Genevet, A., and Tapon, N. (2011) The Hippo pathway and apico-basal cell polarity. *Biochem. J.* **436,** 213–224
4. Zhao, B., Tumaneng, K., and Guan, K. L. (2011) The Hippo pathway in organ size control, tissue regeneration, and stem cell self-renewal. *Nat. Cell Biol.* **13,** 877–883
5. Dong, J., Feldmann, G., Huang, J., Wu, S., Zhang, N., Comerford, S. A., Gayyed, M. F., Anders, R. A., Maitra, A., and Pan, D. (2007) Elucidation of a universal size-control mechanism in *Drosophila* and mammals. *Cell* **130,** 1120–1133
6. Zhou, D., Conrad, C., Xia, F., Park, J. S., Payer, B., Yin, Y., Lauwers, G. Y., Thasler, W., Lee, J. T., Avruch, J., and Bardeesy, N. (2009) Mst1 and Mst2 maintain hepatocyte quiescence and suppress hepatocellular carcinoma development through inactivation of the Yap1 oncogene. *Cancer Cell* **16,** 425–438
7. Overholtzer, M., Zhang, J., Smolen, G. A., Muir, B., Li, W., Sgroi, D. C., Deng, C. X., Brugge, J. S., and Haber, D. A. (2006) Transforming properties of YAP, a candidate oncogene on the chromosome 11q22 amplicon. *Proc. Natl. Acad. Sci. U.S.A.* **103,** 12405–12410
8. Zhao, B., Ye, X., Yu, J., Li, L., Li, W., Li, S., Yu, J., Lin, J. D., Wang, C. Y., Chinnaiyan, A. M., Lai, Z. C., and Guan, K. L. (2008) TEAD mediates YAP-dependent gene induction and growth control. *Genes Dev.* **22,** 1962–1971
9. Lian, I., Kim, J., Okazawa, H., Zhao, J., Zhao, B., Yu, J., Chinnaiyan, A., Israel, M. A., Goldstein, L. S., Abujarour, R., Ding, S., and Guan, K. L. (2010) The role of YAP transcription coactivator in regulating stem cell self-renewal and differentiation. *Genes Dev.* **24,** 1106–1118
10. Strano, S., Monti, O., Pediconi, N., Baccarini, A., Fontemaggi, G., Lapi, E., Mantovani, F., Damalas, A., Citro, G., Sacchi, A., Del Sal, G., Levrero, M., and Blandino, G. (2005) The transcriptional coactivator Yes-associated protein drives p73 gene-target specificity in response to DNA Damage. *Mol. Cell* **18,** 447–459
11. Zhao, B., Wei, X., Li, W., Udan, R. S., Yang, Q., Kim, J., Xie, J., Ikenoue, T., Yu, J., Li, L., Zheng, P., Ye, K., Chinnaiyan, A., Halder, G., Lai, Z. C., and Guan, K. L. (2007) Inactivation of YAP oncoprotein by the Hippo pathway is involved in cell contact inhibition and tissue growth control. *Genes Dev.* **21,** 2747–2761
12. Zhao, B., Li, L., Tumaneng, K., Wang, C. Y., and Guan, K. L. (2010) A coordinated phosphorylation by Lats and CK1 regulates YAP stability through SCF(β-TRCP). *Genes Dev.* **24,** 72–85
13. Lapi, E., Di Agostino, S., Donzelli, S., Gal, H., Domany, E., Rechavi, G., Pandolfi, P. P., Givol, D., Strano, S., Lu, X., and Blandino, G. (2008) PML, YAP, and p73 are components of a proapoptotic autoregulatory feedback loop. *Mol. Cell* **32,** 803–814
14. Ura, S., Nishina, H., Gotoh, Y., and Katada, T. (2007) Activation of the c-Jun N-terminal kinase pathway by MST1 is essential and sufficient for the induction of chromatin condensation during apoptosis. *Mol. Cell. Biol.* **27,** 5514–5522
15. Takahashi, S., Ebihara, A., Kajiho, H., Kontani, K., Nishina, H., and Katada, T. (2011) RASSF7 negatively regulates pro-apoptotic JNK signaling by inhibiting the activity of phosphorylated-MKK7. *Cell Death Differ.* **18,** 645–655
16. Drabløs, F., Feyzi, E., Aas, P. A., Vaagbø, C. B., Kavli, B., Bratlie, M. S., Peña-Diaz, J., Otterlei, M., Slupphaug, G., and Krokan, H. E. (2004) Alkylation damage in DNA and RNA. Repair mechanisms and medical significance. *DNA Repair* **3,** 1389–1407
17. Ringvoll, J., Nordstrand, L. M., Vågbø, C. B., Talstad, V., Reite, K., Aas, P. A., Lauritzen, K. H., Liabakk, N. B., Bjørk, A., Doughty, R. W., Falnes, P. Ø., Krokan, H. E., and Klungland, A. (2006) Repair deficient mice reveal mABH2 as the primary oxidative demethylase for repairing 1meA and 3meC lesions in DNA. *EMBO J.* **25,** 2189–2198
18. Hirayama, J., Sahar, S., Grimaldi, B., Tamaru, T., Takamatsu, K., Nakahata, Y., and Sassone-Corsi, P. (2007) CLOCK-mediated acetylation of BMAL1 controls circadian function. *Nature* **450,** 1086–1090
19. Bao, Y., Nakagawa, K., Yang, Z., Ikeda, M., Withanage, K., Ishigami-Yuasa, M., Okuno, Y., Hata, S., Nishina, H., and Hata, Y. (2011) A cell-based assay to screen stimulators of the Hippo pathway reveals the inhibitory effect of dobutamine on the YAP-dependent gene transcription. *J Biochem.* **150,** 199–208
20. Ogryzko, V. V., Schiltz, R. L., Russanova, V., Howard, B. H., and Nakatani, Y. (1996) The transcriptional coactivators p300 and CBP are histone acetyltransferases. *Cell* **87,** 953–959
21. Suzuki, H., Fukunishi, Y., Kagawa, I., Saito, R., Oda, H., Endo, T., Kondo, S., Bono, H., Okazaki, Y., and Hayashizaki, Y. (2001) Protein-protein interaction panel using mouse full-length cDNAs. *Genome Res* **11,** 1758–1765
22. Yang, X. J., and Seto, E. (2008) The Rpd3/Hda1 family of lysine deacetylases. From bacteria and yeast to mice and men. *Nat. Rev. Mol. Cell Biol.* **9,** 206–218
23. Yamamori, T., DeRicco, J., Naqvi, A., Hoffman, T. A., Mattagajasingh, I., Kasuno, K., Jung, S. B., Kim, C. S., and Irani, K. (2010) SIRT1 deacetylates APE1 and regulates cellular base excision repair. *Nucleic Acids Res.* **38,** 832–845
24. Levy, D., Adamovich, Y., Reuven, N., and Shaul, Y. (2008) Yap1 phosphorylation by c-Abl is a critical step in selective activation of proapoptotic genes in response to DNA damage. *Mol. Cell* **29,** 350–361
25. Tomlinson, V., Gudmundsdottir, K., Luong, P., Leung, K. Y., Knebel, A., and Basu, S. (2010) JNK phosphorylates Yes-associated protein (YAP) to regulate apoptosis. *Cell Death and Disease* **1,** e29
26. Ota, M., and Sasaki, H. (2008) Mammalian Tead proteins regulate cell proliferation and contact inhibition as transcriptional mediators of Hippo signaling. *Development* **135,** 4059–4069
27. Gu, W., and Roeder, R. G. (1997) Activation of p53 sequence-specific DNA binding by acetylation of the p53 C-terminal domain. *Cell* **90,** 595–606
28. Boyes, J., Byfield, P., Nakatani, Y., and Ogryzko, V. (1998) Regulation of activity of the transcription factor GATA-1 by acetylation. *Nature* **396,** 594–598
29. Thompson, P. R., Kurooka, H., Nakatani, Y., and Cole, P. A. (2001) Transcriptional coactivator protein p300. Kinetic characterization of its histone acetyltransferase activity. *J. Biol. Chem.* **276,** 33721–33729
30. Wang, C., Fu, M., Angeletti, R. H., Siconolfi-Baez, L., Reutens, A. T., Albanese, C., Lisanti, M. P., Katzenellenbogen, B. S., Kato, S., Hopp, T., Fuqua, S. A., Lopez, G. N., Kushner, P. J., and Pestell, R. G. (2001) Direct acetylation of the estrogen receptor alpha hinge region by p300 regulates transactivation and hormone sensitivity. *J. Biol. Chem.* **276,** 18375–18383
31. Li, K., Wang, R., Lozada, E., Fan, W., Orren, D. K., and Luo, J. (2010) Acetylation of WRN protein regulates its stability by inhibiting ubiquitination. *PLoS One* **5,** e10341
32. Jang, E. R., Choi, J. D., and Lee, J. S. (2011) Acetyltransferase p300 regulates NBS1-mediated DNA damage response. *FEBS Lett.* **585,** 47–52

33. Vassilopoulos, A., Deng, C. X., and Chavakis, T. (2010) Crosstalk between the DNA damage response, histone modifications, and neovascularization. *Int. J. Biochem. Cell Biol.* **42,** 193–197
34. Yuan, Z., Zhang, X., Sengupta, N., Lane, W. S., and Seto, E. (2007) SIRT1 regulates the function of the Nijmegen breakage syndrome protein. *Mol. Cell* **27,** 149–162
35. Li, K., Casta, A., Wang, R., Lozada, E., Fan, W., Kane, S., Ge, Q., Gu, W., Orren, D., and Luo, J. (2008) Regulation of WRN protein cellular localization and enzymatic activities by SIRT1-mediated deacetylation. *J. Biol. Chem.* **283,** 7590–7598
36. Oberdoerffer, P., Michan, S., McVay, M., Mostoslavsky, R., Vann, J., Park, S. K., Hartlerode, A., Stegmuller, J., Hafner, A., Loerch, P., Wright, S. M., Mills, K. D., Bonni, A., Yankner, B. A., Scully, R., Prolla, T. A., Alt, F. W., and Sinclair, D. A. (2008) SIRT1 redistribution on chromatin promotes genomic stability but alters gene expression during aging. *Cell* **135,** 907–918
37. Dango, S., Mosammaparast, N., Sowa, M. E., Xiong, L. J., Wu, F., Park, K., Rubin, M., Gygi, S., Harper, J. W., and Shi, Y. (2011) DNA unwinding by ASCC3 helicase is coupled to ALKBH3-dependent DNA alkylation repair and cancer cell proliferation. *Mol. Cell* **44,** 373–384
38. Sedgwick, B., Bates, P. A., Paik, J., Jacobs, S. C., and Lindahl, T. (2007) Repair of alkylated DNA. Recent advances. *DNA Repair* **6,** 429–442

THE JOURNAL OF BIOLOGICAL CHEMISTRY VOL. 287, NO. 11, pp. 8318–8326, March 9, 2012

Involvement of Stress Kinase Mitogen-activated Protein Kinase Kinase 7 in Regulation of Mammalian Circadian Clock*[S]

Received for publication, September 29, 2011, and in revised form, January 11, 2012 Published, JBC Papers in Press, January 20, 2012, DOI 10.1074/jbc.M111.308908

Yoshimi Uchida[‡1], Tomomi Osaki[‡1], Tokiwa Yamasaki[‡], Tadanori Shimomura[‡], Shoji Hata[‡], Kazumasa Horikawa[§], Shigenobu Shibata[§], Takeshi Todo[¶], Jun Hirayama[‡2], and Hiroshi Nishina[‡]

From the [‡]Department of Developmental and Regenerative Biology, Medical Research Institute, Tokyo Medical and Dental University, 1-5-45 Yushima, Bunkyo-ku, Tokyo 113-8510, Japan, the [§]Department of Physiology and Pharmacology, School of Advanced Science and Engineering, Waseda University, Shinjuku-ku, Tokyo 162-8480, Japan, and the [¶]Department of Radiation Biology and Medical Genetics, Graduate School of Medicine, Osaka University, B4, 2-2 Yamada-oka, Suita, Osaka 565-0871, Japan

Background: MKK7 is a kinase involved in the cellular stress response.
Results: MKK7 regulates circadian gene expression and the stability of an essential circadian component in unstressed mammalian cells.
Conclusion: MKK7 functions as a circadian clock regulator.
Significance: Our identification of role of MKK7 in the circadian clock provides insight into the importance of stress-responsive molecules in the maintenance of cellular homeostasis.

The stress kinase mitogen-activated protein kinase kinase 7 (MKK7) is a specific activator of c-Jun N-terminal kinase (JNK), which controls various physiological processes, such as cell proliferation, apoptosis, differentiation, and migration. Here we show that genetic inactivation of MKK7 resulted in an extended period of oscillation in circadian gene expression in mouse embryonic fibroblasts. Exogenous expression in cultured mammalian cells of an MKK7-JNK fusion protein that functions as a constitutively active form of JNK induced phosphorylation of PER2, an essential circadian component. Furthermore, JNK interacted with PER2 at both the exogenous and endogenous levels, and MKK7-mediated JNK activation increased the half-life of PER2 protein by inhibiting its ubiquitination. Notably, the PER2 protein stabilization induced by MKK7-JNK fusion protein reduced the degradation of PER2 induced by casein kinase 1ε. Taken together, our results support a novel function for the stress kinase MKK7 as a regulator of the circadian clock in mammalian cells at steady state.

c-Jun N-terminal kinase (JNK) is a member of the family of mitogen-activated protein kinases (MAPKs), which are ubiquitously expressed and evolutionarily conserved (1, 2). JNK is activated by many types of external stresses, including changes in osmolarity, heat shock, and UV irradiation, and this activity is regulated via the phosphorylation of particular tyrosine and threonine residues located in the kinase domain. JNK phosphorylation is catalyzed by two dual-specificity kinases, MKK4[3] and MKK7, that act in a synergistic manner (3, 4). Although most often activated in response to stress, phosphorylated JNK has been detected in unstressed cultured cells and in isolated mouse tissues, such as the brain (5, 6), indicating the importance of JNK signaling in physiological processes other than cellular stress responses. We previously showed that genetic inactivation of the JNK activator MKK7 in mice resulted in defective hepatocyte proliferation and embryonic lethality (7). In addition, loss of MKK7 in mouse embryonic fibroblasts (MEFs) led to their impaired proliferation, premature senescence, and G_2/M cell cycle arrest (7). These findings indicated that MKK7 is crucial for cell proliferation even in the absence of stress and raised the possibility that the MKK7-JNK pathway might contribute to additional normal biological events.

Circadian clocks are endogenous oscillators that drive the daily rhythms of organisms ranging from bacteria to humans (8, 9). These clocks regulate various biochemical, physiological, and behavioral processes with a periodicity of ~24 h (9). Under natural conditions, circadian rhythms are entrained to this 24-h day by environmental time cues, with light level being the most important (10). The core of the clock mechanism in almost all organisms studied to date is a transcription/translation-based negative feedback loop that relies on positive and negative oscillators (9, 11). In mammals, three basic helix-loop-helix PAS (PER-ARNT-SIM) domain-containing transcription factors, called CLOCK, NPAS2, and BMAL1, constitute the positive elements. CLOCK or NPAS2 heterodimerizes with BMAL1 to form a transcriptionally active complex that binds to E-box elements (CACGTG) present in the promoters of members of the *Period* (*Per*) and *Cryptochrome* (*Cry*) gene families (*Per1*, *-2*, and *-3* and *Cry1* and *-2*). Once the PER and CRY proteins have

* This work was supported by a Grant-in-Aid for Scientific Research on a Priority Area from the Ministry of Education, Culture, Sport, Science, and Technology of Japan and the Ministry of Health, Labor, and Welfare of Japan.
[S] This article contains supplemental Figs. 1–4.
[1] Both authors contributed equally to this work.
[2] To whom correspondence should be addressed. Tel.: 81-3-5803-4658; Fax: 81-3-5803-5829; E-mail: hirayama.dbio@mri.tmd.ac.jp.
[3] The abbreviations used are: MKK, mitogen-activated protein kinase kinase; CHX, cycloheximide; CRE, Cre recombinase; Dex, dexamethasone; DKO, double knockout; ES, embryonic stem; KN, kinase negative; MEF, mouse embryonic fibroblast; NLS, nuclear localization signal; Ab, antibody; WB, Western blot; pTP, phosphorylated threonine-proline.

been translated, they form heterodimers that can then translocate to the nucleus to repress CLOCK (NPAS2)-BMAL1-mediated transcription through direct protein-protein interaction. These interactions then set up the rhythmic oscillations of gene expression that drive the circadian clock.

The functions of various clock proteins, including CLOCK, BMAL1, PER1, PER2, PER3, CRY1, and CRY2, are regulated via phosphorylation by various enzymes, including casein kinase-1 ϵ (CK1ϵ), CK1δ, glycogen synthase kinase-3β (GSK3β), and casein kinase-2 (CK2) (12–14). Genetic studies have revealed the important role this phosphorylation plays in mammalian clock function (12, 13). For example, in the Syrian hamster, the *tau* mutation causing a short period phenotype affects the gene encoding CK1ϵ. CK1ϵ was subsequently demonstrated to phosphorylate PER2 (15), and the short period phenotype of *tau* hamsters was directly linked to their lower rate of CK1ϵ-dependent PER2 phosphorylation. Intriguingly, a defect in CK1ϵ-mediated PER2 phosphorylation has also been implicated in human sleep disorders. For example, familial advanced sleep phase syndrome is associated with a missense mutation in the human *PER2* gene, and the corresponding mutated PER2 protein is less effectively phosphorylated by CK1ϵ *in vitro* than is wild type (WT) PER2 (16). At the molecular level, CK1ϵ-mediated PER2 phosphorylation has been shown to decrease the stability of PER2 protein by promoting its ubiquitination (17, 18). Notably, changes in PER2 stability have been linked to changes in the period length of circadian rhythms (19, 20).

In this study, we present evidence that PER2 may also be regulated by MKK7-JNK-mediated phosphorylation, establishing a role for the stress kinase MKK7 in controlling the mammalian circadian clock. Importantly, we demonstrate that the MKK7-JNK signaling pathway has an effect opposite to that of CK1ϵ-induced PER2 destabilization. Thus, MKK7-JNK signaling may provide a balancing influence on clock protein functions that helps to maintain the normal periodicity of the circadian clock machinery.

EXPERIMENTAL PROCEDURES

Plasmids, Reagents, Cells, and Transfection—An EcoRI fragment of full-length nuclear localization signal-fused CRE recombinase (NLS-CRE) (4) was inserted in the corresponding site of pCLNCX (IMGENEX, San Diego, CA) retrovirus vector, generating NLS-CRE-pCLNCX. A HindIII-EcoRI fragment of Myc epitope was inserted in the corresponding sites of pEGFPN2 (Clontech), generating a Myc-GFP-expressing vector. A mutation was introduced into Myc-PER2/pCS2 using PCR-based site-directed mutagenesis (*Per2S*, 5′-gcaaggccgaggctgtggtgtccctcac-3′; *Per2A*, 5′-gtgagggacaccacagcctcggccttgc-3′). Expression vectors for CK1ϵ and HA-ubiquitin were the kind gifts of Dr. A. Takano-Hayata (Osaka University) and Dr. K. Nakayama (Tokyo Medical and Dental University), respectively. Other plasmids used in this study have been described elsewhere (21, 22).

MEFs, HeLa cells, and 293T cells were grown in Dulbecco's modified Eagle's medium (Invitrogen) supplemented with 10% fetal bovine serum (FBS). ES cells were cultured in DMEM (Invitrogen) containing 15% FBS, 0.1% 2-mercaptoethanol (Sigma), and leukemia inhibitory factor (propagation medium). Cultured cells were transfected with Fugene (Roche Applied Science) according to the manufacturer's protocol. SP600125 and calyculin A were purchased from Calbiochem and Wako Pure Chemical Industries, respectively.

Generation of Stable Reporter Cell Lines and Monitoring of Real-time Luciferase Activity—To obtain lines of $Mkk7^{flox/flox}$ MEFs stably expressing firefly luciferase from a 1.8-kb *Per2* promoter fragment, $Mkk7^{flox/flox}$ MEFs were co-transfected with linearized mouse *Per2* promoter-pGL3basic (7 μg) and pcDNA3.1 (1 μg) vectors. After 1 day in standard culture, 0.5 mg/ml G418 was added, and cultures were selected for 2 weeks. Colonies were picked, and their real-time luciferase activities were determined using a Kronos system (ATTO). Two cell lines that showed robust circadian patterns of luciferase activity were selected for further experimentation.

Antibodies—Antibodies (Abs) recognizing the following proteins were used in this study: Myc (9E10), JNK (sc-571), JNK (sc-137018), CLOCK, and actin (all from Santa Cruz Biotechnology, Inc.); ERK, c-Jun, phosphorylated c-Jun, and phosphorylated JNK (Cell Signaling); CK1ϵ (Abcam); mouse PER2 (Alpha Diagnostic International Inc.); HA (Immunology Consultants Laboratory); and FLAG (Sigma). All other Abs have been described elsewhere (22, 23).

Co-immunoprecipitation—Co-immunoprecipitation assays were performed as described previously with some modifications (22). 293T cells or MEFs were washed twice with phosphate-buffered saline (PBS) and homogenized in binding buffer (150 mM NaCl, 1 mM EDTA, 0.5% Nonidet P-40, 1 mM EGTA, 5% glycerol, and 20 mM Tris-HCl, pH 7.4) containing protease inhibitor mixture tablets. Extracts were clarified by centrifugation for 10 min at 15,000 × *g*, and supernatants were incubated with 15 μl of protein G-agarose beads (GE Healthcare) for 1 h at 4 °C. The bead mixture was centrifuged, and the supernatant was incubated for 12 h at 4 °C with the Abs described in each figure legend plus 20 μl of protein G-agarose beads. The beads were washed three times with binding buffer, boiled in SDS sample buffer, and centrifuged. The supernatant was fractionated by SDS-PAGE and analyzed by Western blotting, as described below.

Western Blotting—Immunoprecipitated materials and total cell extracts obtained as described above were fractionated by SDS-PAGE and transferred electrophoretically onto polyvinylidene difluoride membranes. Membranes were blocked with 2 or 5% nonfat milk and incubated for 10 h at 4 °C with the Abs indicated in each figure legend. The blots were incubated with the appropriate secondary Ab plus peroxidase-conjugated anti-mouse or anti-rabbit IgG Ab (Santa Cruz Biotechnology, Inc.) and developed with the ECL Western blotting detection system (Amersham Biosciences).

Ubiquitination Assay—Myc-PER2 was co-expressed with HA-tagged ubiquitin in 293T cells. The cells were lysed in 1% SDS buffer (1% SDS in TBS), boiled for 10 min, and diluted 10-fold in incubation buffer (1% Triton X-100 in TBS) prior to immunoprecipitation with anti-Myc.

Retroviral Transduction—Retroviruses used in this study were produced using the RetroMax expression system (IMGENEX) according to the manufacturer's instructions.

NLS-CRE was expressed in *Mkk7*$^{flox/flox}$ MEFs using the pCLNCX-NLS-CRE vector, with pMD.G/vsv-g as the enveloping vector. The high infection efficiency (95–100%) of this system was confirmed by infecting MEFs with pCLNCX vector expressing GFP (data not shown).

RESULTS

Genetic Inactivation of Mkk7 Gene Alters Circadian Gene Expression—To investigate whether MKK7 was involved in circadian regulation, we examined cultured cells under conditions that provide a good model of the cell-autonomous circadian oscillation that occurs in mammalian peripheral tissues (24). When cultured human and mouse cells are treated with dexamethasone (Dex), a rhythm of circadian gene expression is entrained (24). To visualize circadian rhythms in cultured MEFs, we used previously generated mice carrying a conditional *Mkk7* allele (*Mkk7*$^{flox/flox}$ mice) (25, 26) to establish cultures of mutant MEFs (*Mkk7*$^{flox/flox}$ MEFs) in which MKK7 could be genetically inactivated by expression of NLS-CRE (Fig. 1*A*, *left*). We then generated two independent lines of *Mkk7*$^{flox/flox}$ MEFs that stably expressed firefly luciferase from a 1.8-kb DNA fragment containing the mouse *Per2* promoter (*Per2-Luc/Mkk7*$^{flox/flox}$ line 1, *Per2-Luc/Mkk7*$^{flox/flox}$ line 2). Retroviral transduction of NLS-CRE resulted in genetic inactivation of MKK7 in both cell lines (Fig. 1*A*, *middle* and *right*). When we treated these cells with Dex and monitored real-time *Per2* promoter-driven luciferase bioluminescence, we found that NLS-CRE-mediated inactivation of MKK7 significantly lengthened the circadian period of bioluminescence in both *Per2-Luc/Mkk7*$^{flox/flox}$ line 1 and *Per2-Luc/Mkk7*$^{flox/flox}$ line 2 MEFs (Fig. 1, *B* and *C*, and supplemental Fig. 1, *A* and *B*). Thus, MKK7 influences circadian gene expression in unstressed cells.

Because MKK7 is a specific activator of JNK (1, 2), we speculated that the altered circadian periodicity we observed following MKK7 inactivation might be associated with impaired JNK function. We therefore examined the effect of MKK7 inactivation on JNK phosphorylation. Previous reports have established that, even in the absence of external stress, cultured cells exhibit a low level of JNK phosphorylation (5, 6), a result we confirmed in our *Mkk7*$^{flox/flox}$ MEFs (Fig. 1*D*, *left*). When we treated *Mkk7*$^{flox/flox}$ MEFs with the phosphatase inhibitor calyculin A, JNK phosphorylation was markedly increased. However, when MKK7 was genetically deleted, JNK phosphorylation was significantly reduced both in untreated and calyculin A-treated MEFs (Fig. 1*D*, *right*), showing that the stress-independent JNK activation observed in cultured cells depends on the kinase activity of MKK7. We then examined the effect of the kinase inhibitor SP600125 (which blocks JNK activity) on circadian gene expression and found that SP600125 treatment lengthened the circadian period of bioluminescence in both *Per2-Luc/Mkk7*$^{flox/flox}$ line 1 and 2 MEFs (supplemental Fig. 2). Importantly, the effects of SP600125 on circadian gene expression were strikingly similar to those of MKK7 genetic inactivation (Fig. 1, *B* and *C*). In addition, our results are consistent with previous studies showing that SP600125 extends the period of circadian transcription in cultured cells and in *ex vivo* organ culture systems (6, 27). Thus, our findings provide evidence

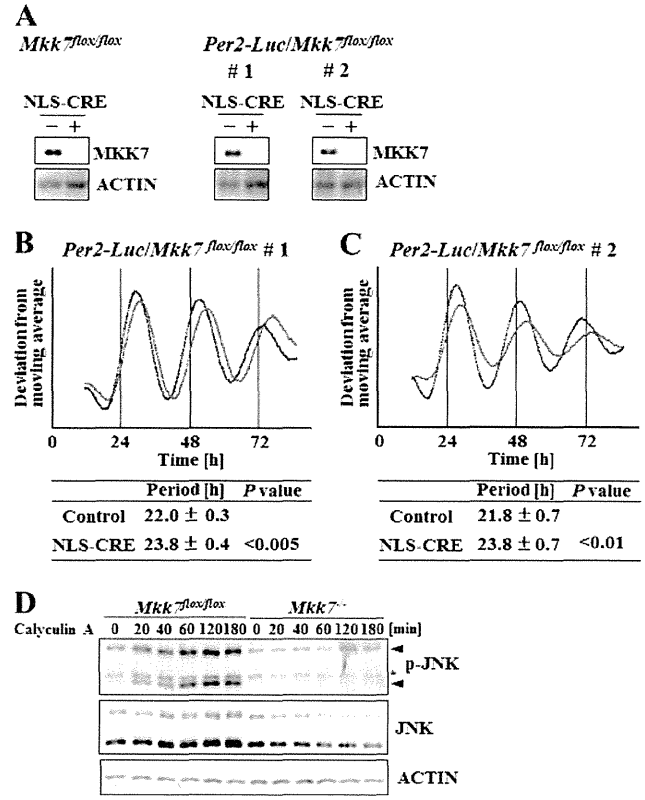

FIGURE 1. **MKK7 controls circadian gene expression in cultured cells.** *A*, confirmation of loss of MKK7 expression. *Mkk7*$^{flox/flox}$ MEFs and two lines of *Mkk7*$^{flox/flox}$ MEFs expressing luciferase under the control of the *Per2* promoter (*Per2-Luc/Mkk7*$^{flox/flox}$ line 1 and *Per2-Luc/Mkk7*$^{flox/flox}$ line 2), were infected with NLS-CRE-expressing (+) or control (−) retroviral vectors. MKK7 levels were determined by WB with anti-MKK7 Ab. *ACTIN*, loading control. *B* and *C*, loss of MKK7 alters the circadian period. *Per2-Luc/Mkk7*$^{flox/flox}$ line 1 (*B*) and *Per2-Luc/Mkk7*$^{flox/flox}$ line 2 (*C*) MEFs were infected with retrovirus expressing NLS-CRE or control vector and synchronized by Dex treatment. *Per2* reporter bioluminescence was monitored over the indicated time course. Detrended data representative of three independent experiments are shown in the *upper panels*. *Blue trace*, control bioluminescence rhythm; *red trace*, bioluminescence rhythm in the absence of MKK7. *Tables* in the *lower panels* show the calculated periods of bioluminescence rhythms expressed as the mean ± S.D. ($n = 3$). *p* values as compared with the control are indicated. *D*, effects of calyculin A treatment on JNK phosphorylation. *Mkk7*$^{flox/flox}$ MEFs infected with NSL-CRE-expressing retrovirus (*Mkk7*$^{-/-}$) or empty vector (*Mkk7*$^{flox/flox}$) were treated with 5 nM calyculin A. At the indicated time points, lysates were analyzed by WB using anti-phospho-JNK (*p-JNK*), anti-JNK (*JNK*), and anti-actin (*ACTIN*) Abs. *Black arrowheads*, phosphorylated JNK. *, nonspecific band. For all experiments, results shown are representative of at least three independent trials.

that the MKK7-JNK signaling pathway is involved in the circadian regulation of gene expression.

MKK7-JNK Fusion Protein Induces PER2 Phosphorylation—To identify the MKK7-JNK target(s) involved in regulating the mammalian circadian clock, we overexpressed an MKK7-JNK (WT) fusion protein in 293T or HeLa cells and performed Western blotting (WB). It has been previously demonstrated that expression of this MKK7-JNK (WT) fusion protein, but not of a kinase-negative (KN) version (MKK7-JNK (KN)), results in *trans*-phosphorylation of JNK by the fused MKK7 and a subsequent marked increase in JNK catalytic activity (21). Consistent with these results, we found that phosphorylation of endogenous c-Jun, a well known JNK target (1), was strongly induced

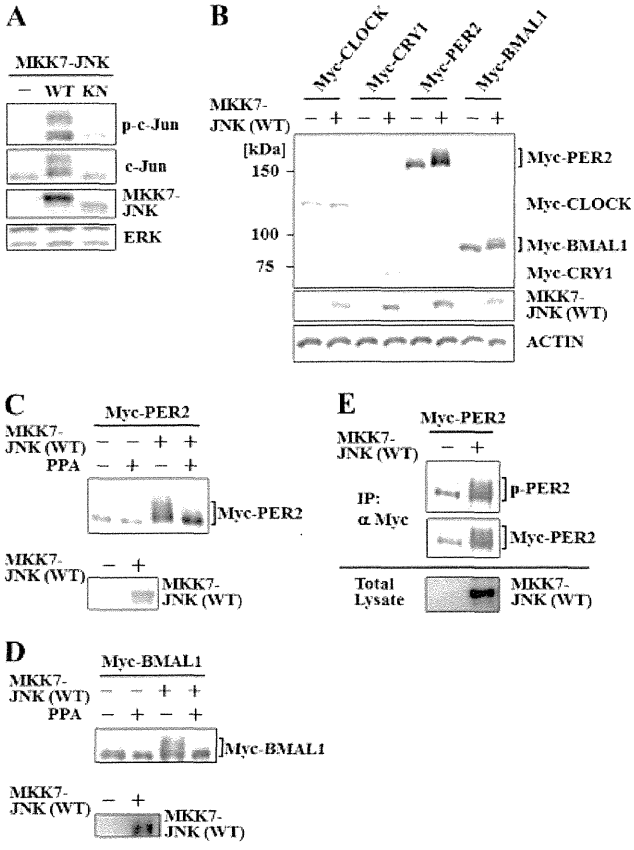

FIGURE 2. **Co-expression of MKK7-JNK fusion protein induces the phosphorylation of exogenous PER2 and BMAL1.** *A*, confirmation of kinase properties. 293T cells were transiently transfected with vectors expressing MKK7-JNK (WT) or MKK7-JNK (KN), and lysates were analyzed by WB with anti-phospho-c-Jun (*p-c-Jun*), anti-c-Jun, anti-JNK, and anti-ERK Abs to detect phospho-c-Jun, c-Jun, MKK7-JNK, and ERK proteins, respectively. Only MKK7-JNK (WT) expression resulted in phosphorylation of the JNK target c-Jun (*p-c-Jun*). *B*, mobility shift of clock proteins. MKK7-JNK (WT) or empty control vector (−) was co-expressed in HeLa cells with vectors expressing Myc-CLOCK, Myc-CRY1, Myc-PER2, or Myc-BMAL1. Lysates were analyzed by WB with anti-Myc Ab to detect the indicated Myc-tagged clock proteins or with anti-JNK Ab to detect MKK7-JNK protein. *Brackets* indicate the shift in the PER2 and BMAL1 bands induced by co-expression of MKK7-JNK (WT). *C* and *D*, sensitivity to phosphatase. HeLa cells were co-transfected with vectors expressing Myc-PER2 (*C*) or Myc-BMAL1 (*D*), plus either empty vector (−) or vector expressing MKK7-JNK (WT) (+). Lysates were treated (+) or not (−) with alkaline phosphatase (*PPA*) and analyzed by WB with anti-Myc Ab to detect Myc-PER2 or Myc-BMAL1 and with anti-JNK Ab to detect MKK7-JNK (WT). *E*, MKK7-JNK-mediated increase in PER2 pTP motifs. 293T cells transiently expressing Myc-PER2 were co-transfected with empty vector (−) or MKK7-JNK (WT) (+). Lysates were immunoprecipitated (*IP*) using anti-Myc Ab to isolate PER2. This immunoprecipitate was subjected to WB analysis with anti-pTP Ab to detect phosphorylated PER2 (*p-PER2*) (*top*) and with anti-Myc Ab to detect Myc-PER2 (*middle*). *Bottom*, WB analysis of total cell lysate using anti-JNK Ab to detect MKK7-JNK (WT).

by overexpression of MKK7-JNK (WT) but not by MKK7-JNK (KN) (Fig. 2*A*). We then examined the effect of MKK-JNK (WT) on the co-expression of a set of Myc-tagged clock proteins. Interestingly, MKK7-JNK (WT) caused a significant shift in the electrophoretic mobility of Myc-PER2 and Myc-BMAL1 (Fig. 2*B*) that could be reversed by phosphatase treatment (Fig. 2, *C* and *D*). These data indicate that JNK-mediated phosphorylation can induce a mobility shift in clock proteins, implying a concrete interaction between MKK7-JNK signaling and the clock machinery.

A particular threonine-proline motif is a consensus site for JNK phosphorylation (28). We overexpressed Myc-PER2 or Myc-BMAL1 in the presence or absence of MKK7-JNK (WT) in cultured cells and examined whether these proteins were phosphorylated on this motif. We immunoprecipitated Myc-tagged clock proteins with anti-Myc Ab followed by WB analysis using an Ab specifically recognizing proteins bearing the phosphorylated threonine-proline (pTP) motif. We found that PER2 was modestly phosphorylated on its threonine-proline motif(s) in control cells but that this PER2 phosphorylation was greatly enhanced by MKK7-JNK (WT) (Fig. 2*E*). However, no band corresponding to BMAL1 phosphorylation was detected in either control or MKK7-JNK (WT)-expressing cells (data not shown). We therefore speculated that PER2 is the more likely circadian target of MKK7-JNK signaling and thus focused our subsequent analyses mainly on PER2.

JNK Physically Interacts with PER2—We tested whether JNK could physically interact with clock proteins using co-immunoprecipitation assays. First, we co-expressed FLAG-JNK with Myc-PER2, Myc-BMAL1, or Myc-LacZ (negative control) in 293T cells and subjected lysates to immunoprecipitation with anti-FLAG Ab. We found that these exogenous forms of PER2 and BMAL1 both co-immunoprecipitated with FLAG-JNK (Fig. 3*A*). To confirm an interaction between PER2 and JNK at the endogenous level, we used anti-PER2 Ab to immunoprecipitate endogenous PER2 from Dex-synchronized WT MEFs at various time points and performed WB to detect endogenous JNK. Indeed, endogenous JNK co-immunoprecipitated with endogenous PER2 in a manner that appeared to depend on the abundance of PER2 protein (Fig. 3*B*).

MKK7-JNK Signaling Stabilizes PER2 Protein—During the course of the above experiments, we realized that MKK7-JNK (WT) expression increased the abundance of PER2 protein, suggesting that MKK7-JNK signaling might affect PER2 stability. To test this possibility, we co-expressed increasing amounts of MKK7-JNK (WT) with Myc-PER2 and Myc-GFP in 293T cells and detected a dose-dependent increase in PER2 protein (Fig. 4*A*). This PER2 up-regulation was almost entirely dependent on the enzymatic activity of JNK because it was not observed when Myc-PER2 was co-expressed with MKK7-JNK (KN). A more modest increase in Myc-PER2 protein was observed in HeLa cells expressing MKK7-JNK (WT) (data not shown), indicating that this phenomenon varies by cell type. We believe that the MKK7-JNK-induced increase in PER2 protein is not due to an elevation in *Per2* mRNA because MKK7-JNK co-expression did not affect levels of Myc-GFP protein (Fig. 4*A*), whose transcription was controlled by the same CMV promoter as that controlling *Per2*.

We next investigated the effect of MKK7-JNK (WT) on the half-life of PER2 protein. To this end, we co-transfected cultured cells expressing Myc-PER2 plus Myc-GFP with empty vector, MKK7-JNK (WT), or MKK7-JNK (KN) and treated the cells with cycloheximide (CHX) to prevent new protein synthesis. Intriguingly, MKK7-JNK (WT), but not MKK7-JNK (KN), markedly extended the half-life of Myc-PER2 protein (Fig. 4, *B* and *C*). Thus, the PER2 protein stabilization attributable to MKK7-JNK (WT) depends on the kinase activity of JNK.

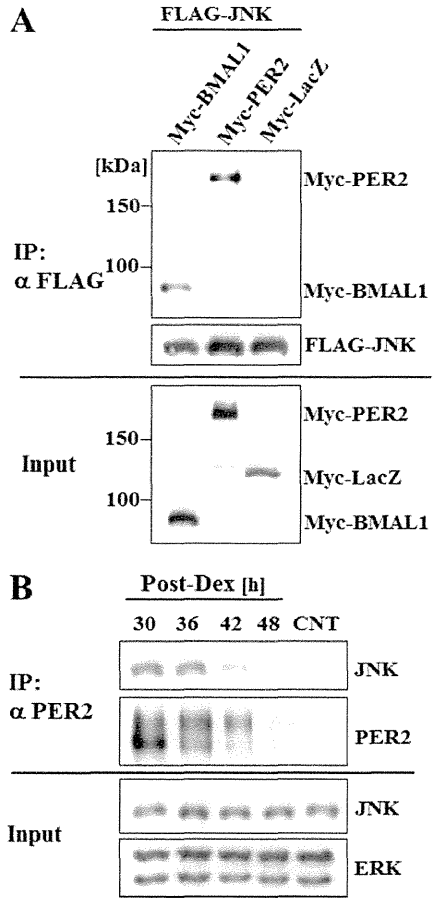

FIGURE 3. **PER2 and BMAL1 can physically interact with JNK.** *A*, exogenous level. FLAG-JNK was co-expressed with Myc-BMAL1, Myc-PER2, or Myc-LacZ in 293T cells. Lysates were immunoprecipitated (*IP*) with anti-FLAG Ab and analyzed by WB with anti-Myc Ab to detect clock proteins or with anti-JNK (sc-571) Ab to detect JNK. *Input*, total lysates subjected to WB with anti-Myc Ab. *B*, endogenous level. WT MEFs were synchronized with Dex, and protein extracts were prepared at the indicated times (h). *Top*, extracts were immunoprecipitated with anti-PER2 Ab, and the immunoprecipitate was analyzed by WB with anti-JNK or anti-PER2 Abs. CNT, Immunoprecipitation using rabbit IgG (negative control). *Input*, total lysates subjected to WB with anti-JNK or anti-ERK Abs.

We previously established mouse ES cells bearing disruptions of both the *Mkk4* and *Mkk7* genes (MKK-DKO ES cells) (29). Because the circadian machinery is not functional in ES cells (30), we can study this cell type to avoid the effects of time-dependent regulation of clock protein expression and degradation. We confirmed that JNK phosphorylation, and therefore activity, was markedly diminished in MKK-DKO ES cells (Fig. 4*D*), consistent with our previous report (29). Interestingly, PER2 protein was also dramatically reduced in MKK-DKO ES cells. In contrast, the expression of other clock proteins, including CLOCK, BMAL1, and CRY1, was comparable in WT and MKK-DKO ES cells. These data support our results obtained using the MKK7-JNK fusion protein (Fig. 4, *A* and *B*) and indicate that JNK activity has a specific effect on PER2 protein stability.

Ubiquitination is an important step in the targeting of PER2 protein for proteasomal degradation (17, 18, 23). We therefore tested the effect of MKK7-JNK (WT) or MKK7-JNK (KN) expression on PER2 ubiquitination. Myc-PER2 was co-expressed in cultured cells with HA-ubiquitin plus empty vector, MKK7-JNK (WT), or MKK7-JNK (KN). Immunoprecipitation of extracts followed by WB showed that Myc-PER2 underwent prominent ubiquitination in control cultures (Fig. 4*E*), consistent with previous reports (17, 18, 23). Significantly, this ubiquitination of Myc-PER2 was efficiently inhibited by co-expression of MKK7-JNK (WT) but not by co-expression of MKK7-JNK (KN) (Fig. 4*E*). These results imply that the enzymatic activity of MKK7-activated JNK is required to block PER2 ubiquitination.

MKK7-JNK Inhibits CK1ε-mediated PER2 Degradation—It has been reported that CK1ε phosphorylates PER2 and induces subsequent PER2 degradation via ubiquitination (17, 18). We found that overexpression of CK1ε caused a significant shift in the mobility of PER2 protein that was consistent with its destabilization (Fig. 5, *A* (compare *lanes 1–3* with *lanes 4–6*) and *B*). This electrophoretic retardation resulted from phosphorylation because it could be reversed by phosphatase treatment (supplemental Fig. 3), a finding consistent with previous reports (17, 18). Notably, co-expression of MKK7-JNK (WT) did not inhibit the electrophoretic retardation of the PER2 protein band induced by CK1ε. Instead, MKK7-JNK (WT) caused an additional shift in the PER2 band (Fig. 5*C*) that was also reversed by phosphatase treatment (supplemental Fig. 3). These data suggest that CK1ε and JNK do not compete in phosphorylating PER2. To confirm this hypothesis, we mutated the Ser-659 residue of mouse PER2 protein to alanine (PER2 (S659A)), thereby altering the residue that corresponds to the best-characterized CKIε phosphorylation site of the human PER2 protein (16). We found that MKK7-JNK (WT) was still able to efficiently phosphorylate the PER2 (S659A) protein (Fig. 5*D*), indicating that MKK7-JNK phosphorylates PER2 at amino acid residue(s) other than Ser-659. When we assessed the effect of MKK7-JNK (WT) expression on CK1ε control over PER2 stability, we found that the enzymatic activity of JNK reduced the destabilization of PER2 induced by CK1ε (Fig. 5, *A* (compare *lanes 4–6* with *lanes 10–12*) and *B*). Furthermore, MKK7-JNK (WT) co-expression suppressed CK1ε-induced PER2 ubiquitination (Fig. 5*E*). Thus, our results clearly show that the MKK7-JNK signaling pathway and CK1ε activity oppose each other in regulating PER2 protein stability.

DISCUSSION

Previous studies have shown that phosphorylation levels of JNK, and thus its kinase activity, fluctuate in a circadian manner in both the suprachiasmatic nucleus, the site of the master clock, and in cultured mammalian cells (5, 6). In addition, the use of the JNK inhibitor SP600125 and siRNA-mediated suppression of *Jnk* have both been reported to lengthen the period of circadian transcription in cultured cells and in *ex vivo* organ culture systems (6, 27, 31). These findings have provided evidence of the involvement of the JNK signaling pathway in circadian regulation. However, several laboratories, including ours, have demonstrated that SP600125 suppresses the activities of kinases other than JNK, such as phosphatidylinositol 3-kinase and Cdk1 (32, 33). Thus, to examine circadian gene expression in the specific absence of JNK activity, we used